

Holographic Video: Design and Implementation of a Display System

by

Mary Lou Jepsen

Bachelor of Science in Electrical Engineering
Brown University
1987

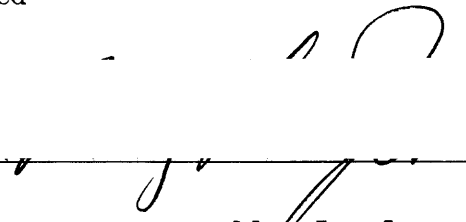
Submitted to the Media Arts and Sciences Section
in Partial Fulfillment of the Requirements of the Degree of
Master of Science

at the Massachusetts Institute of Technology

June 1989

©Massachusetts Institute of Technology 1989
All Rights Reserved

Signature of the Author



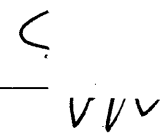
Mary Lou Jepsen
Media Arts and Sciences Section
May 5, 1989

Certified by



Stephen A. Benton
Professor of Media Technology
Thesis Supervisor

Accepted by



Stephen A. Benton
Chairman
Departmental Committee on Graduate Students

Rotch

1

MASSACHUSETTS INSTITUTE
OF TECHNOLOGY

OCT 23 1989

LIBRARIES

Holographic Video: Design and Implementation of an Interactive Display

by

Mary Lou Jepsen

Submitted to the Media Arts and Sciences Section on May 5, 1989 in partial fulfillment of the requirements of the degree of Master of Science

Abstract

A 3-D holographic video system is described. The work on the system to date is detailed. Emphasis is placed on the efforts of the past academic year (1988-89). These efforts were focused around improving the quality of the output medium, commonly referred to as the holographic television set.

Thesis Supervisor: Dr. Stephen A. Benton
Title: Professor of Media Technology

*The work reported herein was supported by
USWest Advanced Technologies.*

Acknowledgments

Without the following people this document would not exist. I would like to acknowledge each one of them for their help:

Stephen Benton for his advice, concern, and wonderful anecdotes, but especially for teaching me more than even he probably realizes. Pierre St. Hilaire for a great deal of help on the project and for being a great friend. John "Pasteurizer" Underkoffler for all of the input images, eloquent words and Mahler. Joel Kollin for his incredible persistence and help. William Parker for insight and the ability to make everything appear within one's grasp. Julie Walker for holding everything together and teaching me so much about it all. Mike Halle for always being so understanding and enlightening and just an all-around amazing person. Mike Klug for being so practical and funny. Larisa Matejic for a fresh perspective and a wonderful database program from which the bibliography was derived. Mark Lucente for all the stories and for being cool and fun. Hiroshi Yoshikawa and Akira Shirakura for teaching me some Japanese and for being so amazingly accommodating and fun.

I'd like to acknowledge the following significant technical help from people outside of SPI: Massimo Russo, Steve Strassmann, Dave Dyer of Symbolics, and Dale Curtis of Lincoln Laser. Thanks also to Doc Edgerton for the use of his "Strobette".

Additionally, without the following friends this thesis would not have been so enjoyable: Megan Smith for listening and actually understanding most of the time. Kevin Landel for a totally different point-of-view. Henry Holtzman for liking fast loud guitars too. Kenji Taima for being scum-cool and for humor. Alan Lasky for making me laugh and laugh and laugh. Dave Small for growing up in practically the same town as me. Peg Schafer for just being great. Sylvain Morgaine for all the rap sessions. And everyone else at the Media Lab: they have all contributed to my wonderful experience here.

I'd also like to thank the following people: Hendrik Gerritsen for letting me into that first holo class in 1983, and for putting faith in me ever since. Taleen Ghazarian, Scott Parlee, and Greg Bowen for being the best engine buddies anyone could have. My family for dealing with me for all these years. And so many countless bands for their inspiration throughout the years.

Additional thanks go to the Multi-Scanning Corporation and General Scanning for their respective donations of a polygonal mirror and a scanning galvanometer, and last, but far from least, I'd like to especially thank US West Advanced Technologies for supporting this research.

Contents

1	Introduction	8
1.1	Historical Perspective	8
1.2	The Historical Development of Holography	9
1.3	Overview of Thesis Goals	13
2	Background	15
2.1	Input Devices	15
2.1.1	Holographic Cameras	15
2.1.2	Holography Without Vibration Isolation	16
2.1.3	Range Finding Cameras	18
2.2	Computer Generated Holograms (CGH)	19
2.2.1	Basics of Computer Generated Holography	19
2.2.2	The Space-Variant DFT for Cell Oriented Holograms	22
2.2.3	Computer Generated Off-Axis Holograms	23
2.2.4	Detour Phase Holograms	24
2.2.5	Method Delay Sampling	27
2.2.6	n -Phase Holograms	27
2.2.7	Nondetour Phase Holograms	27
2.2.8	The Kinoform	28

2.2.9	The ROACH	28
2.3	Three-Dimensional Display of CGHs	29
2.3.1	The Ping Pong Approximation	29
2.3.2	Direct Convolution	30
2.3.3	Born Approximation	30
2.3.4	Multiple Perspectives	31
2.4	The Display Medium	32
2.4.1	Spatial Light Modulators	32
2.4.2	History of Television	34
2.4.3	The Scopphony System	36
3	The MIT Holographic Video System	43
3.1	Goals	43
3.2	Bandwidth Reduction	44
3.3	Parallel Processing Algorithms For Real-Time CGH	46
3.3.1	Generalized Algorithm	47
3.3.2	The Chunky Style Algorithm	48
3.3.3	The Spaghetti Style Algorithm	48
3.4	Design and Information Considerations	49
3.4.1	Interface Requirements	49
3.4.2	Optical Engineering	49
3.4.3	System Performance and Recommendations	52
3.5	The Proposal For This Thesis	52
4	System Improvements	55
4.1	Introduction	55
4.2	The Frame Buffer	56

4.3	Control	57
4.4	Converging Reference Beam	59
4.5	3-D Implementation	59
4.6	System Flexibility	60
4.7	Larger Window/Faster Frame Rate	60
4.8	Computational Issues	61
4.9	Distortion Correction	64
4.10	Additional Improvements	64
5	Theoretical Analysis	67
5.1	Introduction	67
5.2	Analysis of Present System	67
5.3	Proposed Elimination of Electro-Mechanical Parts	74
5.3.1	The Optical Design	77
5.4	Stereogram-Type Video Systems	78
6	Conclusions	84
6.1	Improvements	84

List of Figures

2.1	A Cell of The Detour Phase Hologram Depicting How Phase Delay Is Achieved	26
2.2	The Nipkow Disc	35
2.3	The Original Scophony Television Design	39
2.4	Scophony System without Electro-Mechanical Components	41
3.1	The MIT Holographic Video System as of May, 1988	50
4.1	Re-Positioning Error From Frame t to Frame $t + 1$	58
4.2	The Current Configuration of the Holographic Video Display Device .	66
5.1	The Holographic Video System (Simplified for Mathematical Analysis)	68
5.2	New Holographic Video Setup Using 18 Sided Polygon	73
5.3	AM Envelope Detection	75
5.4	Proposed Elimination of Electro-Mechanical Parts	76

Chapter 1

Introduction

1.1 Historical Perspective

Holography today is at the level of sophistication that photography reached 100-125 years ago. Holographers today must build their own holographic cameras, and these cameras must be completely rebuilt everytime a holographer decides to record a different type of scene. Minor modifications are always necessary when the subject matter is varied in the least; minor modifications in the camera usually require only a few hours of time. A major change in the setup could take days, and sometimes weeks, to debug completely. Many holographers make their own photo-sensitive emulsions, and all must actually process their own holograms. It is a time-consuming process. Speeding up this process is very desirable.

It would be wonderful if the famous **Star Wars** scene were actually possible. In this scene the robot R2-D2 projects out an animated hologram of Princess Leia: She says "Help me Obi-Won-Kanobi..." and then visual and audible static fade in as the image and voice fade out. This was a great special effect; so much so that much of the public believes that holography has reached this state. The animated holographic figurines depicted on **Star Trek: The Next Generation** are another example.

Holographic video has been depicted in many motion pictures, television shows, and science fiction novels. However, such a medium does not yet exist. This thesis tracks the early development of a holographic video system being developed at the MIT Media Lab. This existing system is far from the level of sophistication expected when one hears the term "holographic video". To date, only images containing a small number of points have been successfully transmitted. However, the foundation of the work thus performed is firm. The potential of the system is promising.

Holographic video has reached the level of sophistication that television reached 80 years ago: as such, there is much room for improvement, and luckily, no transmission standards have yet been set. It will be sometime before the quality of the system reaches the state where the implementation of standards can be considered. Much experimentation can therefore occur. But, let the discussion begin with a short review of the historically significant developments in the discipline of holography itself.

1.2 The Historical Development of Holography

In most conventional light recording techniques like photography, a flat picture of a 3-D scene is recorded onto a light-sensitive surface. This feat is accomplished with the use of a lens, or at least a pinhole (ie the camera obscura). The resultant recording is derived only from the amplitude distribution of the original scene. All information pertaining to the relative phases of the light arriving at the photo-sensitive plate is lost.

What makes holography different from conventional photography is holography's ability to record the complete wave field: both the amplitude and phase of the waves of light hitting the photo-sensitive material. The phase information can be converted into variations in amplitude if a coherent overlapping reference beam is used.

This conversion is necessary because of the lack of phase sensitive recording materials. Through the use of coherent illumination, and the introduction of a coherent reference wavefront to interfere with the light reflected by the object, the phase information is transferred into amplitude information, and is recorded on the film. The intensity at any point depends upon both the amplitude and phase of the object wave. The developed photographic image bears no direct resemblance to the object of the holographic setup: the amplitude and phase information is indirectly encoded. The hologram can be decoded via illumination once again with the reference beam; the object wavefront is then reconstructed. A viewer peering through the hologram will perceive this object wave as identical to the original object wave. The viewer will see a 3-D image with all the cues to depth that the object would exhibit if it were physically there.

Holography was invented by Dennis Gabor in 1948 [1]. He was able to make small and noisy holograms of 2-D transparencies at this time, but the advent of the continuous wave He-Ne laser (1962) made the practice of holography much more practical. A major flaw with the holograms made by Gabor was the presence of an unwanted twin image. E. Leith and J. Upatnieks in the early 1960's eliminated this extra image by using an off-axis reference beam [2]. A spatial carrier frequency was introduced by using a separate reference wavefront incident upon the photographic plate at an appreciable angle. The effect of this off-axis reference beam angle was the separation of the two images by a large enough angle from the directly transmitted beam and from each image to insure that the images did not overlap. Additionally, with the laser, Leith and Upatnieks were able to make holograms of solid objects with appreciable depth[3].

At the same time, the Russian holographer Y. N. Denisyuk developed reflection holography [4], [5]. In this form of holography, the object and reference beams are incident upon the photographic emulsion from opposite sides. The interference fringes

recorded in such a process form developed layers nearly parallel to the surface of the emulsion and half a wavelength apart. As a result, reflection holograms are similar to Lippmann photographs and exhibit very strong color selection: the 3-D image these holograms project is monochromatic.

This early work by Leith, Upatnieks, and Denisyuk in the area of holography sparked the interest of the scientific community. Research in the areas of holographic multiple imaging, imaging through diffusing and aberrating media, computer generated holograms, the production and correction of holographic optical elements, and holographic interferometry was subsequently conducted by scientists throughout the world.

Investigation of holographic 3-D display resulted in the production of life-size holograms, portraits with pulsed lasers and multi-color images. Little further progress was made until Benton invented the rainbow hologram in 1969 [6]. This was a transmission hologram in which vertical parallax was sacrificed in order to gain the ability to illuminate the hologram with white light, and the ability to create a bright single color image. This initial invention led Benton to develop new and better techniques for both multi-color and achromatic holography. Additionally, the rainbow hologram led to the development of the white-light stereogram [7].

The stereogram today, in 1989, is gaining commercial importance. Stereograms have found useful applications in areas such as CAD-CAM design, medical imaging, air-traffic control, art, and portraiture [8]. The average turnaround time from 3-D database to complete stereogram is currently several weeks. However, if a standard format was established, the turn around time could be significantly reduced, although it might still take several days to go from 3-D database to a final hologram. For some applications, this amount of time is not significant; other applications require nearly instantaneous 3-D imaging.

A product designer could make use of an instantaneous 3-D imager, such as a holographic video system, as a peripheral attachment to a CAD/CAM design system. When the designer wished to inspect an aspect of his design that called for the creation of a real physical model, he would have an option. Rather than sending some drawings to the prototype department and waiting weeks for a model to be built, he could simply print out a 3-D hologram. This would allow the designer to perceive subtleties that go unnoticed in a 2-D representation of his design. The concept-to-prototype time lag could be significantly reduced.

The advantages of a fast turnaround time in the field of medical imaging are obvious; life threatening situations require ~~expedience~~^{expediting}. The better the quality of the image, the more the doctor can deduce about the status of his patient. A 2-D, low resolution X-ray delivers *some* information *quickly*. The same is true of MRI and CAT-scan data. This information is low-quality in the sense that the data presented is in the cryptic form of 2-D "slices" from the volume being imaged. If the data was processed and presented in a holographic format, this data could not only be more quickly understood, but aspects not apparent in the 2-D slices would become obvious. For example, aneurysms in blood vessels could be perceived in holographic format with ease. These aneurysms might go undetected in the more conventional viewing format. If such holograms could be created as quickly as X-ray films, the doctor would have access to valuable information pertaining to the status of his patient.

Air traffic controllers *need* to know where all the planes in the vicinity of an airport are at all times. A holographic video system setup in the control tower would make this requirement an easy task to accomplish. 2-D radar screens currently in use do not give enough information to allow one to quickly comprehend situations. For example, planes that appear to be colliding on the 2-D radar screen may, in fact, merely be overlapping one another: in actuality the planes may be flying at different altitudes. A holographic video system would make this fact apparent in a quick glance.

For holography to be of greater utility, the time involved in transforming a 3-D database or real physical object into a final hologram demands reduction. The practice of holography has evolved since the days of Gabor; high quality holograms of objects that have never physically existed are now possible through the use of the computer. The process of making these holograms even more quickly might also be accomplished via electronic means. Movie film requires at least a few hours to process; video, however, is ready for viewing almost immediately. Perhaps a holographic video system, being driven by the powerful computers available today, can reduce the time involved in making a hologram into a regime where they can be more useful. The fields of product design, medical imaging, and air traffic control would directly benefit.

Unfortunately, no recording medium with both the resolution of holographic film and the speed of conventional video exists [9]. This harsh reality has prolonged, but not completely impeded, the development of a holographic video system.

1.3 Overview of Thesis Goals

This thesis traces the development of the world's first holographic video system. The project responsible for developing this system has been ongoing for the past 2 years; emphasis in this document is placed on the improvements made over the past year.

Chapter 2 details the background and history necessary to understanding the decisions made in creating the MIT holographic video system. A survey of possible input and output devices, and a brief history of both computer generated holography and television is thus given. Chapter 3 documents the progress made during the first year of the MIT holographic video project. Parallel processing algorithms were devised

and a basic display system was defined. Improvements and modifications made to this system over the past year are detailed in Chapter 4, and a theoretical analysis of the entire system as well as proposals for new systems are given in Chapter 5. Chapter 6 outlines and summarizes the document and emphasizes the importance of certain details.

Chapter 2

Background

2.1 Input Devices

The holographic video system of the future demands a holographic camera for recording, a holographic television set for display, and video processing equipment to connect these two devices. The requirements for the camera will be examined first.

2.1.1 Holographic Cameras

The idea of creating a holographic camera is not new. Most holographic setups are designed with production of a hologram depicting a specific object. Because the lighting of this object is crucial to the quality of the hologram, it is necessary to alter the lighting for new objects placed in this setup. This alteration entails changing the reference beam(s) intensity, direction(s) and subsequently retuning a quantity referred to as *path length*. The art of balancing the object and reference beams in the holographic setup becomes an iterative process. This balancing requires the precise movement of many the components involved in the setup. A camera possessing an abundance of moving parts and the ability to calculate the location required by these

parts is difficult to manufacture. Some holographic cameras have been introduced that allow *some* lighting control, however, the latitude in most cases is poor, relative to the latitude that one has when one build one's own setup from "scratch". For this reason, it is still traditional in holography to construct a new setup for each object. Additionally, the components in most setups must be vibrationally isolated. The object of this holographic setup must also be vibrationally isolated. This requirement excludes all living, moving creatures from becoming the subject matter of this type of hologram: these subjects vibrate.

2.1.2 Holography Without Vibration Isolation

It is possible to make holograms of subjects that do not require any vibration isolation. This feat may be accomplished in either of two ways.

Holograms Made With Pulsed Lasers

One method employs a powerful laser capable of reducing the exposure time required into the nanosecond regime [10]. In this regime, vibration and movements that would normally prevent the achievement of standing waves, and therefore a hologram, are effectively motionless. The effect is analogous to the use of a strobe light to "freeze" a gymnast in mid air. These lasers are referred to as pulsed lasers. They eliminate the requirement of vibration isolation, but the necessity of this process being carried out on in a darkened room remains. The need for a video-rate recording medium with the resolution of holographic film also remains.

Holographic Stereograms

Another way to create holograms of non-vibrationally isolated volumes is through the stereographic approach [11]. Here, a movie camera slides along a track in front of the person or object that will act as the subject of the ultimate hologram. The camera takes anywhere from 2 to 300 or more pictures as it moves across this track. These pictures are recorded at evenly spaced intervals along the track. The object must stay reasonably still, to allow for continuity between the photographs. The camera takes n perspective views of a 3-D scene. The developed film is then inserted into a cinema-type projector on a vibrationally isolated table. Laser light is used as the light source in this projector. The developed film's image is projected onto a light diffusing screen. It is this image that acts as the object of the holographic exposure. The introduction of a reference beam allows the encoding of each image into a thin slit on the holographic film. The presence of the object and reference wavefronts allows interference to occur, and the phase information of the light to be recorded. The rightmost view is encoded into a slit on the rightmost edge of the holographic plate. The second rightmost view is encoded into the slit that is abutted against that rightmost slit, and so this process continues until the entire holographic plate has been exposed, one slit at a time.

The stereogram approach requires both a very dark room and vibration isolation. However, these parameters aren't required for the actual recording of the object being holographically imaged. The extraction of a 3-D database from the recorded camera data and the use of this information to compute the interference fringes of the hologram would result in holograms of non-vibrationally isolated, physically existing objects. Additionally, the computer could be used to actually create a scene, a 3-D database, that never physically existed. The hologram could then be computed from that 3-D database.

2.1.3 Range Finding Cameras

Much work has been done in the MIT Media Laboratory and elsewhere regarding the subject of range finding cameras. These cameras extract a 3-D database from a scene. V. Michael Bove Jr. in his PhD thesis explains many different schemes for accomplishing this extraction [12]. The use of one stationary camera was favored. The camera may move; but the camera doesn't *have* to move, in particular the camera needn't move on a specific track as is required in stereogram recording. The reflectance of a line of laser light sweeping over the scene was measured. From the intensity of the reflected light field, the distance the wavefront had traveled and the shape of the reflecting surface were determined. The major flaw with this method is the difficulty in recording an entire 3-D database. Surfaces obscured from the camera can not be recorded, and thus volumes can not be computed in these regions. Prediction algorithms were incorporated into this work; they were successful in determining a high percentage of "unknown" volume. Paul Linhardt worked with Bove and used a 2 camera stereo approach to extracting the 3-D database. Even the 2 camera approach left a great deal of volume obscured. However, 2 cameras can reveal more information than one. After the prediction algorithms were implemented, the difference between the 2 camera and 1 camera approach was deemed insignificant. The one camera method emerged as the preferred choice, due to its simplicity.

Another range finding camera approach emerged at the same time as the one described above. This camera was able to extract depth from focus. It used a lens that was constructed to allow for two separate optical paths. The focal lengths of the optical paths were identical, however the apertures differed resulting in different depths of focus for each path. It was possible to extract a 3-D database from this information.

2.2 Computer Generated Holograms (CGH)

Using the 3-D input from the natural world, or a 3-D database created directly by the computer, it is possible to compute the actual interference pattern that would be created by placing a physical representation of this database into a holographic setup.

2.2.1 Basics of Computer Generated Holography

The formation of a computer generated holographic image can be divided into 4 steps.

- The object must be chosen.
- The wave front of that object must be calculated.
- This wavefront must be encoded into a hologram transmittance.
- The scene is reconstructed from the hologram transmittance.

Simplification of the calculations involved in computer generated holography can be accomplished by careful choice of the object. A Gabor hologram uses a single diverging beam transmitting through a 2-D transparency at distance z from the hologram recording plane. This type of hologram yields a Fourier relationship between the complex-amplitude transmittance of the hologram and the reconstructed image of the 2-D transparency [13], [14]. This sort of setup has been used almost exclusively by researchers in the field of computer generated holography. A review of what has been accomplished in this endeavor is presented.

If light propagation is represented by a parabolic approximation, and a constant multiplicative factor is ignored, then points on the hologram can be described in terms

of the reduced coordinates:

$$\mu = \frac{-x}{\lambda z_0}; \nu = \frac{-y}{\lambda z_0}. \quad (2.1)$$

Here, λ refers to the wavelength of light involved in making the hologram, x and y are coordinate axes parallel to the object plane and z is the coordinate axis perpendicular to the object plane. z_0 is the distance to the plane of the hologram. The complex amplitude resulting at $z = z_0$ from a CGH with complex amplitude transmittance $\tilde{v}(\mu, \nu)$ at $z = 0$ is

$$v_1(x, y) = \exp \frac{i\pi(x^2 + y^2)}{\lambda z_0} \iint \tilde{v}(\mu, \nu) \exp[2\pi i(\mu x + \nu y)] d\mu d\nu. \quad (2.2)$$

$$= \exp\left[\frac{i\pi(x^2 + y^2)}{\lambda z_0}\right] v(x, y). \quad (2.3)$$

Except for the quadratic phase factor, the complex amplitude at z_0 is the Fourier transform of the hologram transmittance [15]. This factor is ignored because it is the intensity, $|v_1(x, y)|^2$, that is usually recorded in holography. By varying z_0 the scale of the reconstruction is varied: no other effect is accrued. The wavefront using the reconstruction geometry described above is:

$$\tilde{u}(\mu, \nu) = \int_{-\infty}^{+\infty} \int_{-\infty}^{+\infty} u(x, y) \exp[-2\pi i(\mu x + \nu y)] dx dy. \quad (2.4)$$

To compute the complex amplitude transmittance digitally, as is customary when using a computer, the transformation must be taken at a set of discrete points. The most obvious method involves restricting attention to a set of points in the object $u(x, y)$ separated by distances $(\delta x, \delta y)$ in the x and y directions respectively. Then:

$$u_{mn} = u(m\delta x, n\delta y), \quad (2.5)$$

$$-(M/2) \leq m \leq (N/2) - 1, \quad (2.6)$$

$$-(N/2) \leq n \leq (N/2) - 1. \quad (2.7)$$

The bounds are derived from the finite extent of the object:

$$M\delta x = \Delta x, \quad N\delta y = \Delta y, \quad (2.8)$$

$$M \times N = \text{number of points in the object.} \quad (2.9)$$

M and N can also be odd; only minor modifications to these calculations need to be made in that event. Sampling the hologram, then, at distances

$$\delta\mu = \frac{1}{\Delta x}, \quad (2.10)$$

$$\delta\nu = \frac{1}{\Delta y}, \quad (2.11)$$

the wavefront described in Equation 2.4 can now be rewritten as:

$$\tilde{u}\left(\frac{j}{\Delta x}, \frac{k}{\Delta y}\right) = \sum_{m=-M/2}^{(M/2)-1} \sum_{n=-N/2}^{(N/2)-1} u_{mn} \exp[-2\pi i(mj/M) + (nk/N)], \quad (2.12)$$

where:

$$-M/2 \leq j \leq ((M/2) - 1), \quad (2.13)$$

$$-N/2 \leq k \leq ((N/2) - 1). \quad (2.14)$$

Fast algorithms exist for computing this discrete Fourier transform (DFT) depicted in Equation 2.12 [16]. The object wave at the hologram is the Fourier spectrum. Encoding the distribution is accomplished via either a cell-oriented or point oriented approach.

The surface of a cell-oriented hologram is arranged into small rectangular units called resolution cells. A point-oriented hologram can be described as the result of a point nonlinearity acting on a continuous object wavefront at the hologram. The continuous wave front is either known or obtained from interpolation of the DFT.

Object Constraints

The object consists of $M \times N$ points. This number is referred to as the space-bandwidth product of the hologram [17]. It is invariant with magnification. The space-bandwidth product of the Fourier spectrum is equal to the space-bandwidth product of the object [17]. The complexity of the hologram is directly related to the complexity of the object and vice-versa.

2.2.2 The Space-Variant DFT for Cell Oriented Holograms

The complex amplitude transmittance of the $(j, k)th$ resolution cell is $\tilde{C}_{jk}(\mu, \nu)$; this quantity is not necessarily constant over the cell. The transmittance over one period of the hologram cell is:

$$\tilde{T}(\mu, \nu) = \sum_{j=-M/2}^{(M/2)-1} \sum_{k=-N/2}^{(N/2)-1} \tilde{C}_{jk}(\mu - j\delta\mu, \nu - k\delta\nu). \quad (2.15)$$

The transmittance of the entire hologram is then:

$$\tilde{T}_e(\mu, \nu) = \sum_{p=-\infty}^{\infty} \sum_{q=-\infty}^{\infty} \tilde{T}(\mu - p\Delta\mu, \nu - q\Delta\nu). \quad (2.16)$$

The inverse Fourier transform of this is:

$$T_e(x, y) = T(x, y)(\Delta\mu\Delta\nu)^{-1} \sum_{m=-\infty}^{\infty} \sum_{n=-\infty}^{\infty} \delta(x - \frac{m}{\Delta\mu})\delta(y - \frac{n}{\Delta\nu}) \quad (2.17)$$

$$= \sum_m \sum_n \delta(x - \frac{m}{\Delta\mu}) \delta(y - \frac{n}{\Delta\nu}) T_{mn} \quad (2.18)$$

The relative complex amplitude of the (m, n) th reconstructed image point is

$$T_{mn} = (\Delta\mu\Delta\nu)^{-1} T(\frac{m}{\Delta\mu}, \frac{n}{\Delta\nu}). \quad (2.19)$$

And the inverse Fourier Transform of Equation 2.15 then yields

$$T(x, y) = \sum_j \sum_k C_{jk}(x, y) \exp[2\pi i(j\delta\mu x + k\delta\nu y)]. \quad (2.20)$$

Substituting from Equation 2.19 yields:

$$T_{mn} = (MN)^{-1} \sum_j \sum_k C_{jk}^{mn} \exp(2\pi i(\frac{jm}{M} + \frac{kn}{N})) \quad (2.21)$$

$$C_{jk}^{mn} = (\delta\mu\delta\nu)^{-1} \int_{-\delta\mu/2}^{\delta\mu/2} \int_{-\delta\nu/2}^{\delta\nu/2} \tilde{C}^{jk}(\mu, \nu) \exp(-2\pi i(\frac{m\mu}{\Delta\mu} + \frac{n\nu}{\Delta\nu})) d\mu d\nu. \quad (2.22)$$

Each resolution cell transmittance $C^{jk}(\mu, \nu)$ gives rise to the pseudo-Fourier coefficients C_{jk}^{mn} which are space variant. That is to say, the coefficients vary with position (m, n) in the reconstructed image. To the extent that this space variance can be ignored, the DFT relates the periodic cell-oriented hologram to the reconstructed image: each hologram resolution cell gives rise to one DFT coefficient.

2.2.3 Computer Generated Off-Axis Holograms

Most CGH's have real, non-negative transmittances; such a constraint is applied when one attempts to physically represent a hologram. This constraint implies both that the reconstructed image will have Hermetian symmetry:

$$T_{mn} = T_{-m, -n}^* \quad (2.23)$$

and that T_{∞} will have a considerably larger modulus than any image points surrounding it. The reconstruction will exhibit a twin image and a DC spike. The constraint 2.23 restricts the assignment of values to one half of the object field, $m > 0$ for instance. C^{mn} would then require an $M \times N$ element DFT, but the object can only consist of $[M/2 - 1]N$ points. By changing the extent of the object and evaluating only the real part of the hologram transmittance, $\tilde{\mu}_{jk} = \tilde{A}_{jk} \exp(\tilde{\phi}_{jk})$, the cell transmittance becomes:

$$C_{jk} = K_0 + 2\tilde{A}_{jk} \cos\left(\frac{\pi j}{4} + \tilde{\phi}_{jk}\right) \quad (2.24)$$

This form emphasizes the fact that the discrete hologram is now modulated onto a carrier spatial frequency; it is this carrier frequency which accounts for the off-axis imaging property of the hologram.

2.2.4 Detour Phase Holograms

The first computer generated hologram to actually be created is detailed by Brown and Lohmann in their 1966 article [18]. This first hologram was capable of imaging a 2-D plane rather than a 3-D volume because the algorithm computed Fraunhofer diffraction patterns, not Fresnel diffraction patterns (the type required for creating a 3-D hologram). The CGH is created via the computation of the image's Fourier transform, similar to the process described above. The Fourier transform describes far field diffraction, or Fraunhofer diffraction; this diffraction regime can be used because the image is 2-D and "far" from the area of interest: the plane where the interference is being calculated.

This CGH was called a Detour Phase Hologram. It was a cost-saving approximation that allowed off-axis reconstruction without increasing the hologram space

bandwidth product. The idea was to consider the CGH as a distorted grating, then a wavefront diffracted towards the first order would be advanced or delayed by the distortion in the grating. This distortion was achieved through a displacement of the grating aperture from its normal position (see Figure 2.1). The amount of phase change was proportional to the displacement of the grating aperture; the farther the wave must *detour* from its intended direction, the greater the phase delay.

The Detour Phase Hologram is binary, as there is no gray scale; any given area is either opaque or transparent. As a result this is also an amplitude hologram. The hologram itself is represented with basic units called cells, these are regions of equal size. A cell is divided into 2 apertures whose total width depend on the transform's magnitude. The position of the apertures within the cell are dependent on the computed phase delay for that cell.

The Brown and Lohmann paper was a significant advancement in the field of holography. For the first time, the object of the holographic setup needn't physically exist. Instead, a mathematical model of the object was stored in a computer's memory. This achievement opened a new path for holography.

Difficulties with the Brown and Lohmann Detour Phase Hologram stemmed from some of the approximations made in the algorithm [19] [20]. A detour phase error, associated with the division into cells, caused inhomogeneous image intensity. Quantization error yielded false images. Gap and overlap occurred when the phase exceeded (+) or (-) π . Truncation error also occurred when the hologram was smaller than the spatial extent of the transform.

It was clear that more research was called for.

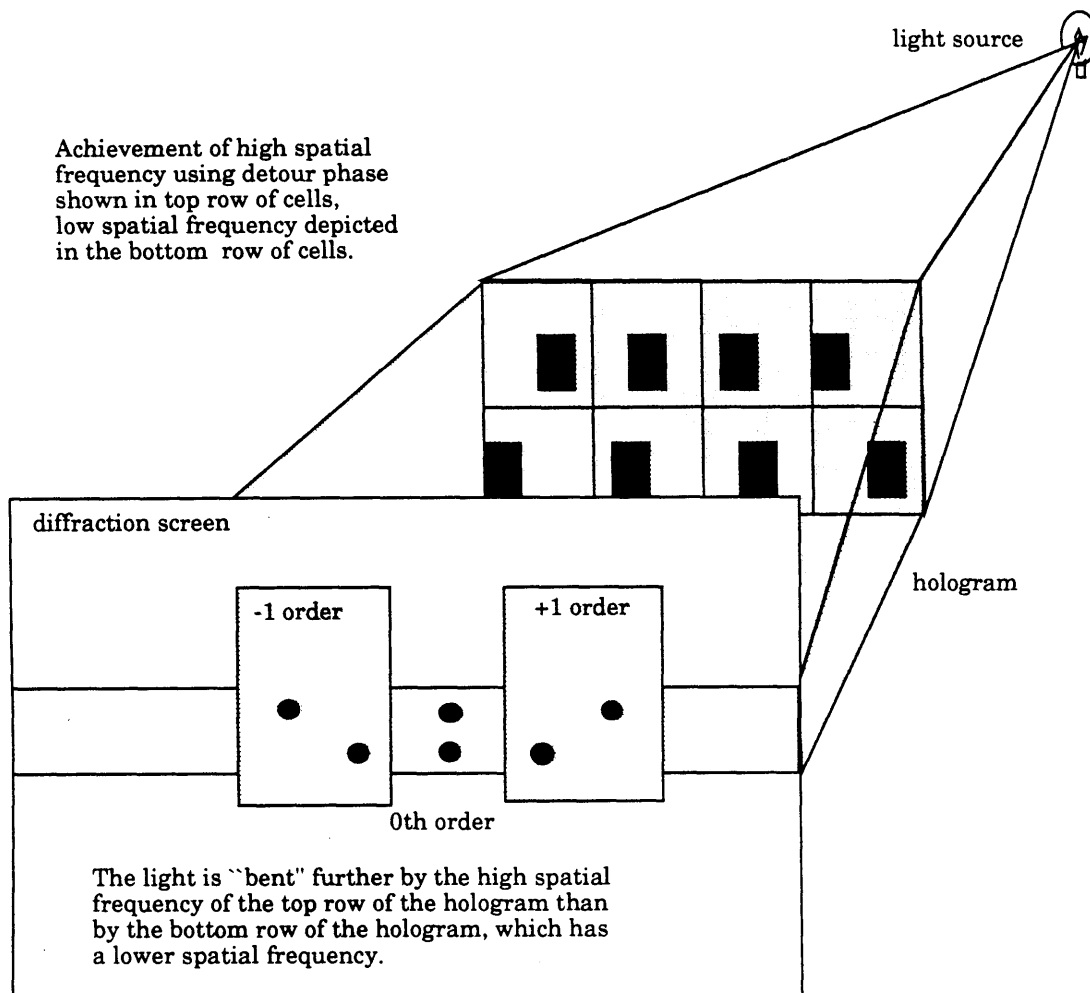


Figure 2.1: A Cell of The Detour Phase Hologram Depicting How Phase Delay Is Achieved

2.2.5 Method Delay Sampling

Lee developed a method that decomposed the Fourier transform of the object into 4 quadrature components [21]. The phase of each component was then coded into discrete functions. The sum of these 4 functions represented the discrete function. Lee called this Method Delay Sampling. The four functions were represented by apertures at 4 laterally displaced positions.

This method simplified the calculations required in obtaining CGHs; no phase quantization is required, because the transmittance of each cell varies. Additionally the vertical sampling rate is one fourth of the the horizontal sampling rate, and thus some limited bandwidth compression has been achieved.

2.2.6 n -Phase Holograms

Hsueh and Sawchuck displaced even and odd diffraction orders with their Double Phase Holograms [22]. The method involved the decomposition of hologram transmittance into two phase quantities. Each cell was divided into two subcells which were vertically separated. The detour phase method therefore displaced diffraction orders vertically.

Burckardt proposed a similar algorithm that used 3 rather than 2 components [23]. The quality of the resultant holograms was improved compared to that previously possible in each case.

2.2.7 Nondetour Phase Holograms

Lee developed a binary computer generated hologram algorithm that didn't use the detour phase concept [24]. His experiments were based on computing the holo-

gram as an interferogram. Fringes were determined by the set of points satisfying inequalities involving the phase of the reconstructed wave. He demonstrated reconstruction of spherical, conical and helical wavefronts. Using these types of holograms he was able to analyze the difficulties with detour phase holograms [25]. The major problems discovered were: the aliasing associated with sampling at discrete points in the hologram plane, and the aliasing that occurred when phase variations exceeded 2π . It is for this reason that the n phase holograms yielded better image quality than other detour phase algorithms.

Burch encoded Fourier sine and cosine transforms of real functions that described objects. This scheme worked far better for on-axis holograms, as the autocorrelation function was lower for on-axis reconstruction than off-axis reconstruction [26].

2.2.8 The Kinoform

The Kinoform is a phase-only hologram, where the phase is implemented by dielectric phase shifting [27]. Dielectric variations in the grating allow light to diffract more efficiently than in an amplitude type grating. The Kinoform assumes that the Fourier spectral modulus of the CGH is constant. This assumption doesn't present a problem if the modulus was originally constant. Such is the case in holographic interferometric applications. In more general CGH cases, the Fourier Spectral Modulus is not constant. However, the distortions accrued are surprisingly small [15].

2.2.9 The ROACH

The ROACH (referenceless on-axis complex hologram) was another important development in the history of computer generated holography [28]. It employed multi-emulsion photographic film (Kodachrome II). One emulsion layer controlled

the transmission modulus, the other controlled the phase modulus.

The proper exposure is achieved by imaging a computer generated pattern from the face of a computer display device, such as a CRT, through two separate color filters, one red and one green, onto the film. The calculation of the CGH can be broken up into 2 steps using these filters. The relation between the intensity displayed and the final complex-amplitude transmittance of the ROACH is usually encoded in the red sensitive layer of the Kodachrome. The complex-amplitude transmittance desired for the reconstructed image is encoded into the green-sensitive layer. The ROACH yields a complex amplitude transmittance even though it allows the reconstructed image to appear on the optical axis. It would certainly prove difficult to attempt the analog of a multi-emulsion film in video format.

2.3 Three-Dimensional Display of CGHs

The holograms previously discussed are capable of imaging a 2-D plane at a given distance z from the hologram itself. Ideally, a CGH would be capable of imaging an entire 3-D volume. This involves the more complex computation of the Fresnel transform, usually by a series of approximations involving the Fourier transform. Progress in this area is outlined.

2.3.1 The Ping Pong Approximation

The "Ping Pong" approximation first represents the object of the holographic setup as a series of 2-D planes. The amplitude distribution at the first plane is propagated to the second plane by a discrete Fourier transform (DFT), multiplied by a quadratic phase factor, and inverse DFTed. The resulting complex amplitude at the

second plane, due to the first plane, is multiplied by the complex amplitude transmittance of the second plane. The process continues for the number of planes in the series. This algorithm has the ability to obscure surfaces, because of a later plane's ability to block light scattered by previous planes. The "Ping Pong" name derives from the fact that one is constantly transforming from one domain back into another domain, and then back again [29].

2.3.2 Direct Convolution

A similar algorithm to the "Ping Pong" approach can be performed when the interplanar distance divided by the hologram's F-number is on the order of one sampling cell. Also, the phase variations from the object must not be rapid, meaning that a series of 2-D planes displaced in depth and depicting rather simple imagery will work well. The point spread function is then limited in spatial extent. Propagation convolution may then be used, because this method involves only a few elements at a time. If the object field is sparse, this approach becomes very economical. Even if the field is very dense, the calculations are still less burdensome than those of the "Ping Pong" approach [15].

2.3.3 Born Approximation

If one now ignores interactions between the planes of the image, an even more economical approach can be used. The various image planes are Fourier-transformed and multiplied by the appropriate quadratic phase factor in order for the transform of each plane to be shifted to its appropriate plane. At the recording plane, the Fourier transforms are added up to create the hologram itself. Only one transform per depth plane is required with this algorithm. If an image in one plane is behind an image in

another plane, the former will shine through the latter; surfaces can not be obscured as with the “Ping Pong” Approach. This algorithm works for imaging transparent and self-luminous objects. The method is based on the Born approximation because there is no secondary field scattering [15].

2.3.4 Multiple Perspectives

The stereogram approach to optical holography has already been discussed. If 3-D scenes could be represented by a series of 2-D perspective views, as is done in the making of stereograms, the amount of information that needs to be computed would be greatly reduced. It is simple to do a Fourier transform to compute the hologram, but the computation becomes more difficult as one moves to a 3-D object. In that case, the Fresnel diffraction regime must be modeled; a Fourier Transform no longer describes this regime. It is often desirable to allow the 3-D image to straddle the plane of the hologram; a Fresnel diffraction model is also capable of modeling in this diffraction regime.

If a series of 2-D perspective views of this 3-D scene are used, rather than a series of 2-D planes displaced in depth or the 3-D database itself, a simplified Fourier transform algorithm may be readily employed. Perceptually, this representation of the object offers much more surface continuity than the representation schemes previously mentioned; note the similarity in object representation to that used in stereograms.

[30] [31]

2.4 The Display Medium

Assuming for the time-being that the hologram computation could be accomplished at video frame rate, a medium to display this 3-D holographic information is then required: a spatial light modulator of very, very high resolution and fast response. The response must be fast enough to display a frame rate of close to 30 Hz. The 30 Hz figure is commonly used in the video industry, and is below the threshold at which most perceive flicker [32]. An animated image composed of a series of slightly displaced 'stills' will appear to be in a natural, continuous and smooth motion if a new still frame is presented every 30th of a second.

2.4.1 Spatial Light Modulators

William Parker's master's thesis documents a widely ranging literature search performed in an attempt to find a suitable spatial light modulator for holographic video [33]. Although a great deal of effort is being placed on the development of spatial light modulators, and the materials that make them up, for a variety of purposes, no entirely suitable medium for holographic video, or even dynamic electronic holography, yet exists.

However, Parker outlines a few different designs for a dynamic electronic holographic display using technologies available today. He cites recent advances in the production of devices with submicron structures and a deeper understanding of electro-optic effects as reasons for optimism. Using microfabrication technology, it is possible to make a linear array with fine enough resolution to serve as one horizontal scan line of the display; this scan line could be multiplexed into a frame via a variety of commercially available scanning methods. The presentation of these frames at video rate, however, would require a very fast response from the electro-optic material being used

to modulate the light. However, frames could be cycled at a rate orders of magnitude faster than possible with conventional photography. Parker refers to this type of display as dynamic electronic holography (DEH) rather than “holographic video” because “holographic video” implies the attainment of a flicker-free presentation of views (an animation). Although the achievement of animation was the eventual goal of Parker’s work, current material constraints forced the present design of a display that could be updated at a slower rate. Improved electro-optic materials will allow Parker’s DEH designs to achieve faster and faster frame rates. Eventually the DEH will attain a response time where displayed animation is possible is possible.

Parker alternatively devises a scheme in which an electron or laser beam could be used to generate the diffractive structure in an electro-optic material. The major problem with this scheme is identical: the slow response of the electro-optic material will not allow a frame composed of these horizontal scan lines to update at video rate. Smectic A, and Smectic C^* chiral liquid crystals have response in the time regime required for the update one horizontal scanline of the holographic video system at 30Hz. However, the speed of the material and the sophistication of scanning technology prevent the simple and direct adoption of these liquid crystal materials to holographic video [33]. Photo-chromics, photo-refractives, thermoplastics, thermochromics, magnetic films, electro-chromics, electrophoretics, and liquid crystals were all investigated. Parker did devise a few schemes for the implementation of a system with a much slower frame rate. One such scheme used a pre-manufactured memory chip, and therefore required no further micro-fabrication nor the associated equipment and facilities. His thesis concluded that there was no obvious way to create an ultra high resolution real-time display capable of updating the amount of information in holograms at 30 frames per second using the technologies he investigated.

It is interesting to note that the pioneers of television itself faced similar problems during the infancy of that medium. Perhaps the clever solutions that these scientists

and engineers devised can offer some insight into the problem at hand.

2.4.2 History of Television

In 1897 Karl Ferdinand Braun developed the Braun Tube. This device was the forerunner to the CRT [34]. It had a fluorescent screen and the ability to deflect an electron beam across this screen. In 1929 Vladimir Zworykin gave the first demonstration of true TV. The pickup was by means of camera tube, the iconoscope, and reproduction was accomplished with a cathode ray tube (CRT) called the kinoscope. Throughout the years the CRT has evolved to its present state. As Parker demonstrated in his thesis, a super high resolution CRT, with a front-end attachment that could transform this modulation into a form where coherent diffraction could occur, is simply not feasible in the near future. However, there were *other* television designs that were not as successful as the CRT, in particular there were many electro-mechanical televisions devised during this time period [35] [36].

The Nipkow disc predates the Braun Tube (1886) and is the best known of these unsuccessful prototypes (see Figure 2.2) [37]. The design calls for a spinning disc with a helical array of holes. The holes are arranged from the center to the edge of the disc in such a way that only one hole at a time sweeps by a small window area where the disc is not obscured from the viewer. Each hole scans one horizontal scanline. One revolution of the disc then scans an entire frame. The large-area light need only be modulated temporally. The disc itself does both the horizontal deflection via the hole translating across the viewing window, and the vertical deflection because each hole sweeps out a different, and vertically displaced, horizontal scanline.

Other electro-mechanical systems were developed prior to 1935, but they all suffered from the same problem as the Nipkow Disc: extremely low light efficiency. The

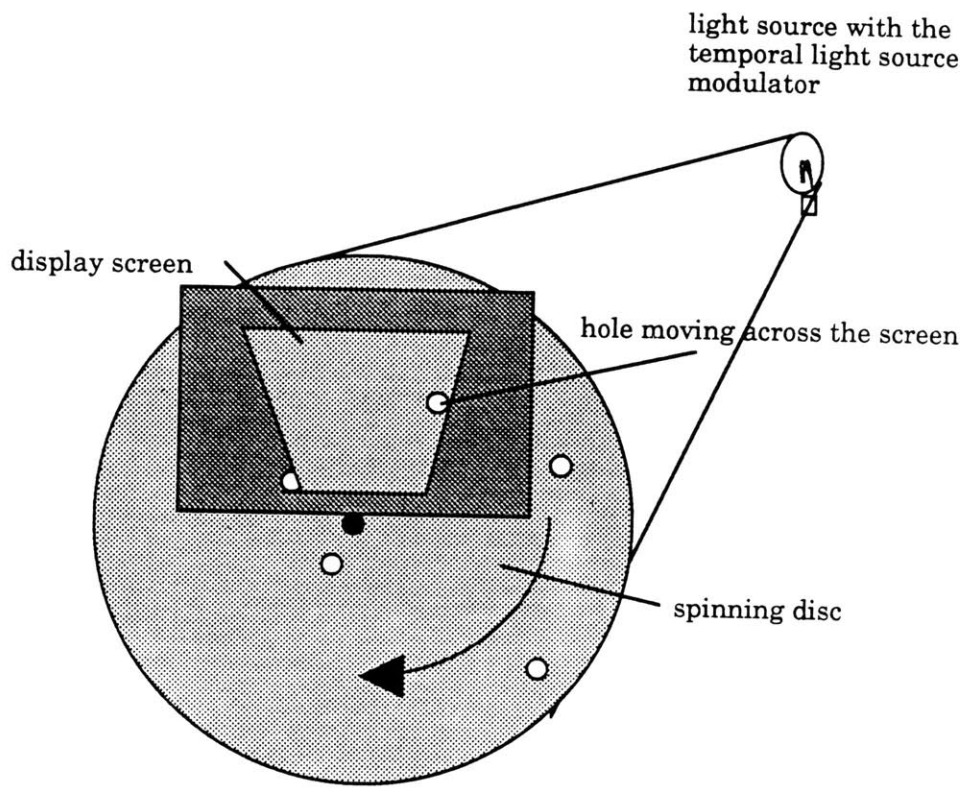


Figure 2.2: The Nipkow Disc

images were dim; ways were sought to improve this condition. [38]

2.4.3 The Scophony System

With 20/20 hindsight, one can look and marvel at the inventions of the Scophony Company [39]. This was a television system circa 1936-1940 that was vying with the cathode ray tube for acceptance as the television display medium of choice: the display around which the standards would be set. The CRT, first demonstrated in 1926, had quite a time lead on the Scophony system, and partly due to this fact; the CRT won the battle. Yet much can be learned from the Scophony system which may be applicable to holographic video: how can one create a huge 2-D array of micron size pixels that can be updated at video rates?

In 1936, Scophony Television Laboratories in Great Britain were the first to tackle the problem from the *optical* point of view, resulting in the evolution of a series of novel optical principles [40]. For instance, the "split-focus" was first devised here. An advance of far-reaching importance was the creation, in conjunction with this optical principle, of what was referred to as the Scophony Supersonic Light Control. Through the use of this light control method the lab devised a television which they called *The Wave-Slot*. In order to understand how *The Wave-Slot* works, a brief description of how ultrasonic acoustic waves can be made visible will be given.

The Acousto-Optic (AO) Effect

An acoustic wave can be characterized by recurring periodic compression and rarefaction of the medium which it traverses through. In an ultrasonic acoustic wave, these differences are more closely spaced than at audible frequencies. The exact spatial frequency of the acoustic wave depends on the speed of sound in the medium

that this wave is traversing, and of course, upon the frequency of the wave itself. As an acoustic wave traverses certain transparent materials, referred to as acousto-optic modulators, the compressions and rarefactions compress and stretch the material enough to significantly change its local refractive index [41].

Light shining through one side of the transparent AO modulator, and perpendicular to the direction of propagation of the acoustic wave, is output at the opposite face. However, these variations in refractive index phase-modulate the transmitting light field. The variations in refractive index mentioned above effect the speed of light and cause the *field* of light to interfere both constructively and destructively at the output. If this output light field is focused via a lens, the result is a diffraction pattern describing the modulation being sent across the AO modulator. This pattern is also referred to as the Fourier transform of the input acoustic signal. After the light comes to a focus, due to the effect of the lens on the wavefront, the field inverts and begins to expand outwardly from the focal point towards an image plane. At the focus, the light is filtered through a "stop" [42]. The variations of refractive index occurring along the AO modulator are expressed as variations in light intensity at the image plane. Thus, an acoustic wave is made visible. It is important to note that this "visible" acoustic wave is still traveling at the speed of sound.

The Fundamental Scanning System

In the Scophony Supersonic Light Control System, this traveling wave is optically slowed to a complete stop. A line scanner, for example a rotating polygon, is introduced into the optical path of the image. The polygon sweeps the image of the AO modulator over an output screen at a speed corresponding to the speed of the acoustic waves but in opposite direction. In this way each element of the acoustic

wave gives a storage of modulation over a considerable length of time:

$$\frac{\text{length of the AO cell}}{\text{velocity of sound}} = \text{the storage of modulation.} \quad (2.25)$$

Additionally, the acoustic wave that travels across the AO modulator now appears to remain still. It is this storage of modulation that accounts for the relatively high efficiency of this device. The system described above is capable of displaying a 1-D visual image. In order to achieve the more conventional two-dimensional video image a vertical scanner is required. A scanning galvanometer is capable of doing the low frequency scanning required for this task (see Figure 2.3). A frame is built up through the addition of many single horizontal "scanlines"; this frame is also "stationary" in the sense that it is a continuously scanned still frame. The ability to change these frames at a minimal rate of 30 frames per second allows the video to become animated. Subtle changes between the information in each frame transform into the appearance of motion across the display, see Figure 2.3 for a complete system diagram.

Chromatic Aberration Correction

Because the continuous wave laser wasn't invented until 1962, the Scophony system had to use white-light arc sources, and had to find a clever way to correct for chromatic aberration in the scanning system. White light incident on a diffractive structure, such as the AO modulator, is broken into a spectrum on the other side of the structure. Red veers the most off course from the original intended direction of the white light; and blue the least. Refractive elements behave oppositely: blue bends the most and red the least. Therefore, Scophony employed refractive prisms in order to compensate for the diffractive effect. Chromatic aberration was eliminated.

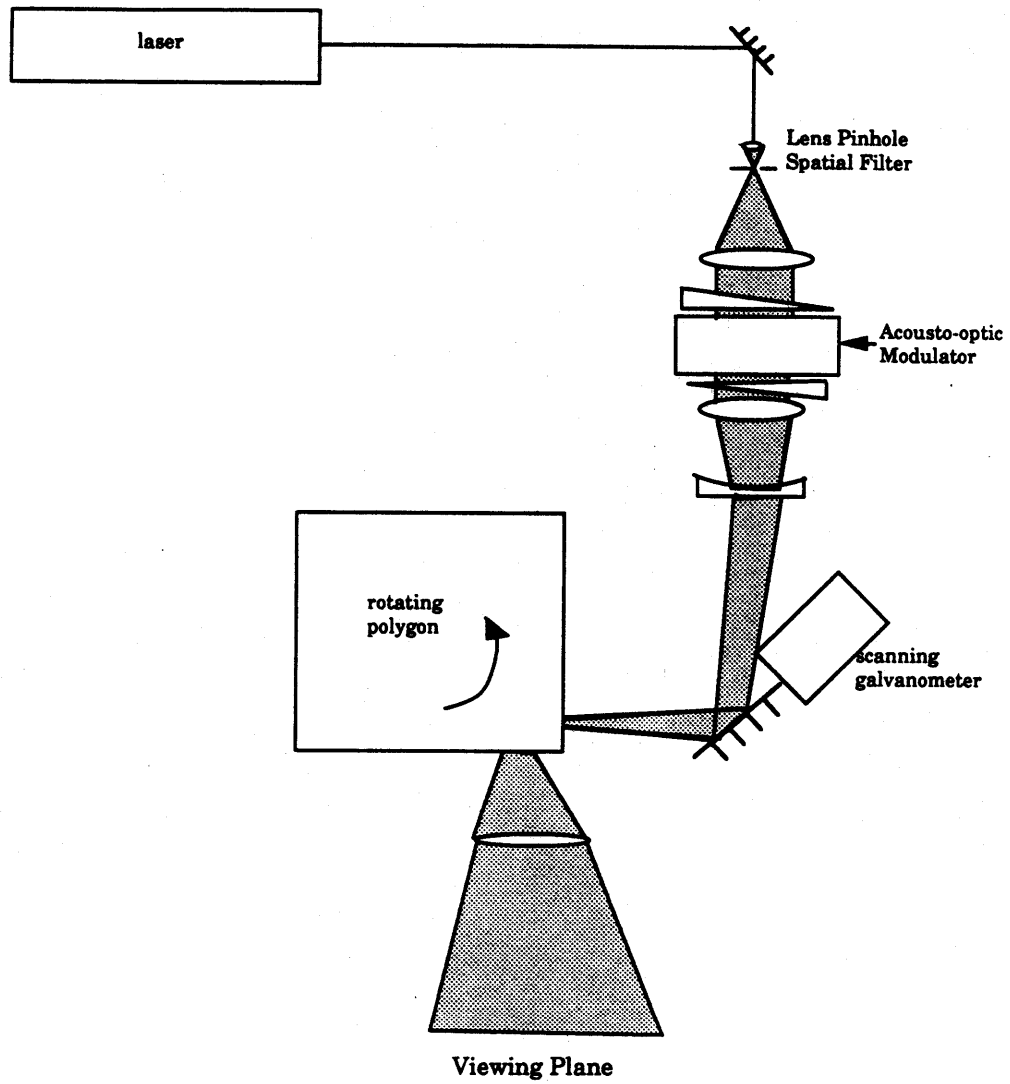


Figure 2.3: The Original Scophony Television Design

Advantages of the Scophony System

The Scophony system was easy to upgrade into a large screen video system. Unlike the cathode ray tube, where the size of the image is limited to the tube size, the Scophony system merely requires more divergent optics and the placement of the screen further away in order to achieve a larger display size. These modifications are easily facilitated. The image is still bright even when spread across a 13 x 10 foot screen; however, the room lights need to be dimmed for this configuration to function well. Scophony yielded significantly brighter images than was possible with conventional "flying spot" scanners. Additionally, the resolution achievable with the flying spot scanner was poor compared to the Scophony system. The system was a very efficient serial to parallel converter. Because the system was capable of handling high speeds, it could translate this ability into high resolution. Other systems not capable of handling information at similar rates couldn't achieve an equivalent density of information.

Elimination of Electro-Mechanical Parts

The Scophony system was criticized as unreliable due to the electro-mechanical components it employed: the rotating polygon and the scanning galvanometer. Improvements were made. Instead of continuing to synchronize the rotating polygon to the speed of the sound wavefront traveling across the AO modulator, one AO modulator was synchronized to a new, second AO modulator, which had been introduced into the setup. High-power electronics were no longer required due to the fact that the motor of the rotating polygon no longer had to be driven. An image is transmitted to the first AO modulator as before, and a signal, a linear frequency ramp, is transmitted to the second AO modulator rather than the rotating polygon. The linear frequency scan received by this second AO modulator counteracts the speed

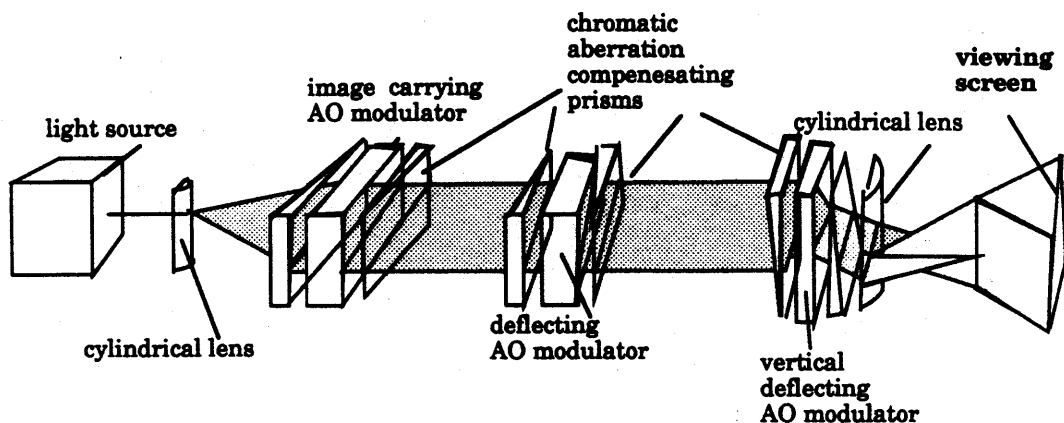


Figure 2.4: Scophony System without Electro-Mechanical Components

of the image traveling across the first AO modulator. The resulting output image is then motionless. A set of these line-images can be made into one 2-D image, a frame. Vertical deflection, like that achieved via scanning galvanometer, is required for this task, and can be achieved with another AO modulator. A frequency ramp spanning a more limited range is transmitted to this AO modulator, which is vertically oriented. The frequency varies much less rapidly than in the horizontally deflecting modulator and duplicates the scanning effect of a scanning galvanometer. (see Figure 2.4)

The advantage of this implementation is the elimination of the mechanical moving parts: the rotating polygon, and the scanning galvanometer. This exclusion makes stability easier to achieve and the system on the whole more reliable.

Through out the years, minor improvements have been made by various scientists

and engineers upon the original Scophony design and the individual components involved. The achievement of higher resolution frames has been documented by many [43], [44], [45], [46], [47], [48]. However, no-one has attempted to achieve the resolution required by holograms using this type of display. In fact, very little work has been done in an attempt to achieve holographic video via any means [33]. However a great body of documented research explores issues in the design, creation and use of 3-D input devices, computer generated holography, and faster, higher resolution, spatial light modulators.

Some of the techniques, materials, and devices encountered in the search through this body of literature can be used in non-obvious ways to create a holographic video system. In actuality, many of the historical ties to the literature were discovered only after the initial system had been designed. The historical references served to prove the validity of the concept rather than to seed the development of the initial design. The presentation of this historical information prior to the system description in this document allows easier comprehension of the thesis. However, the presentation does not accurately reflect the chronological project development. In reality, the Spatial Imaging Group was not aware of the existence of the Scophony system until November, 1988. However, the holographic video system that has evolved resembles the Scophony system to a limited extent. The design and implementation of the holographic video system, the first of its kind, is now described.

Chapter 3

The MIT Holographic Video System

3.1 Goals

Holographic video would bring both realism, and speed and accuracy of perception, to visual communication that surpasses the capabilities of 2-D video systems. Such a system would find great utility in the fields of product design, medical imaging, and air-traffic control. However, the technical difficulties involved in creating such a system have been extreme. The rest of this chapter outlines a new approach to the design of a holographic video system. The rationale as to how reduce the required bandwidth of the transmission channel is discussed. The development of parallel processing algorithms for CGH computation on the Connection Machine is recounted. The display system design and development during the academic year 1987-88 is examined in detail.

3.2 Bandwidth Reduction

A great deal of information exists in an ordinary optical hologram. Fine-grained silver halide emulsions are capable of recording and displaying more than 2000 line pairs per millimeter, corresponding to 4000 pixels/mm [49]. This figure implies 40 gigapixels necessary to make up the 50 mm \times 50 mm display window. Film has a very fine grey scale, generally much finer than the video industry standard of 8 bits/pixel, but this depends upon resolution. In the last chapter, however, many CGH algorithms with only 1 bit/pixel were cited. Eight bits per pixel will significantly reduce the quantization noise accrued with these algorithms. The required bit rate is:

$$40 \frac{\text{gigapixels}}{\text{frame}} \times 8 \frac{\text{bits}}{\text{pixel}} \times 30 \frac{\text{frames}}{\text{second}} = 9.6 \frac{\text{Tera-bits}}{\text{second}}. \quad (3.1)$$

9.6 Tera-bits/sec is quite a fast data rate; optical fibers are capable of transmitting this bandwidth but existing hardware can not adequately process information at this speed. This problem is in addition to the already difficult display problem.

Ways to reduce the bandwidth are required if a holographic video system is to be realized. The fastest, easily adaptable hardware for updating the screen are the high resolution ((1K \times 1K), 8 $\frac{\text{bit}}{\text{pixel}}$, 60 $\frac{\text{frame}}{\text{sec}}$ frame buffers. If the system is to function, the reduction into a regime where computer hardware, such as this extremely fast frame buffer, would be capable of updating frames at video rate is necessary.

Bandwidth reduction factors have been derived from our growing understanding of visual perception, especially that of 3-D information. This knowledge has led to bandwidth reduction through [50]:

- reduction of diffraction angles,
- elimination of vertical parallax.

Additionally, via clever electronic implementation the following can be accomplished [51]:

- reduction of space bandwidth product,
- the elimination of the carrier frequency transmission.

A reduced angle of view can offer a viewing latitude with enough range for good 3-D perception. The computed hologram need only diffract the light through this reduced angular range, about 12 degrees, rather than spanning 30 or more degrees as more conventional holograms. A 12 degree angle corresponds to a spatial frequency of 330 linepairs per millimeter (lp/mm). The equivalent resolution in video industry terms is 660 pixels/mm, a substantial improvement from the 4000 pixels/mm resolution of fine grained silver halide emulsions. Additionally, humans perceive 3-D through the comparison of the two horizontally displaced views seen from the two horizontally displaced eyes. Vertical parallax is not required for 3-D perception, so neither is a resolution of 330 lp/mm in the vertical direction of the holographic display medium. As a result, the amount of information demanded is reduced by a factor of 100. Only enough image resolution to give 2-D vertical information is demanded; 100 vertical divisions are deemed sufficient.

The display must be able to fill both eyes at once. The standard inter-ocular distance is 62 mm. The viewing zone, arbitrarily chosen to be 600 mm from the display plane, is 125 mm wide. This width gives the two eyes an opportunity to perceive a variety of views. Because the hologram itself is 50mm long and 660 pixels per millimeter are required, 33000 pixels per horizontal scan line are demanded. 100 of these scan lines per frame are wanted. The ideal holographic display then is 33000 X 100 and fits into a 50mm X 1mm window, the *holographic image*, as opposed to the hologram itself, is perceived through a 50 mm × 50 mm 2-D window as a 3-D volume. At 8 bits/pixel and 30 frames/sec the required data-rate corresponds to 800

Mbits/sec. Examination of attainable refresh rates employing existing hardware shall now be investigated.

Standard NTSC, the television transmission standard in the USA, updates 640 x 480 pixels at 30 Hz. This corresponds to, at 24 bits per pixel, 180 Mbits/sec. A high resolution display, ie. 1.2K x 1K, 24 bits/pixel, 30 Hz, corresponds to a bit rate of 864 Mbits/sec. This bit rate implies entrance into a range where existing hardware can handle the video transmission problem.

3.3 Parallel Processing Algorithms For Real-Time CGH

Much work has been done by the Spatial Imaging Group on the computation of holograms in real time using the equipment available in the Media Laboratory. John Underkoffler details the work completed as of May 1988 in his bachelor's thesis. More work has been done since then, but the bulk of the research is detailed in the referenced document [52]. Underkoffler's thesis concentrates on the issues involved in simulating the holographic process by using a Connection Machine supercomputer to compute interference patterns at discrete points in a selected hologram plane.

The Connection Machine is a massively parallel supercomputer. A full Connection Machine has 64K microprocessors; each of these has an associated amount of memory which stores numbers and symbols in the form of pvars, or parallel variables. Execution of an instruction upon a pvar is begun from the SIMD (Single Instruction Multiple Data) architecture of the Connection Machine. What is unusual about the Connection Machine is its connectivity. Each processor can communicate with any other processor within 14 cycles, due to an innovative 14-dimensional interconnection scheme. This ability makes the Connection Machine the ideal candidate for certain

classes of problems, among them image processing. For the computation of holograms however, little utility has been found for the interconnectivity of the machine [52]. Each processor simply does its isolated manipulation to the discrete location upon which it is operating.

Unfortunately, the input/output bandwidth on the Media Lab's version of the Connection Machine's hardware was quite low last year. As a result, data transfer in either direction seriously degraded performance. Only when the processors of the CM are kept occupied may the machine's performance approach that of a supercomputer. The I/O bottleneck has since been remedied as the Media Lab received a new model of the Connection Machine in late December 1988.

3.3.1 Generalized Algorithm

The object to be displayed in the hologram is modeled as a collection of self-luminous points sitting both behind and in front of the hologram plane. The points may exist as a continuum of x and z locations but are constrained to lie at discrete y positions corresponding to the positions of the scan lines. No existing CGH algorithms can compute this type of hologram, so Underkoffler devised his own.

He chose to model the physics of holography on the Connection Machine. He elected to compute the interference pattern of two electromagnetic fields, one being a 3-D array of self luminous points making up the the object itself and the other being a plane wavefront. Later this plane reference wave was replaced with a converging wavefront, coming from a slight off-axis direction. Underkoffler dealt with the issues of modulo-phase determination, normalization, and aliasing.

3.3.2 The Chunky Style Algorithm

Underkoffler's "chunky-style algorithm" is a way of fitting our desired holographic window (the 33,000 x 100) pixels into the available 2-D configuration of microprocessors in the Connection Machine. This implementation constrains all source points to be stored in a single pvar. Points in a single row of the pvar must all lie on the same holographic scan line. Worst of all, this type of configuration limits the number of source points available for modeling the object to 128 per scan line, this restriction could pose a problem, depending upon the speed with which I/O can be accomplished. Additionally, the innermost loop, which calculates field amplitudes and adds these to a running total, continues as long as there is at least one scan line which has more source point contributions to be added. Therefore, scan lines which are "ready to go" must sit idle and wait for the other scanlines to finish their computation. This problem led to Underkoffler's design of the Spaghetti Style Algorithm.

3.3.3 The Spaghetti Style Algorithm

This algorithm configures the Connection Machine in its linear mode, rather than in the "chunky-style" algorithm where the CM was configured to operated on a 2-D array. In the linear approach one long scan line is worked upon. This long line can later be chopped up into several shorter horizontal scanlines placed in a 2-D array. This approach is faster because it doesn't require as great a setup time as the "chunky style" approach. Underkoffler additionally explored the feasibility of a number of other algorithms that he ultimately abandoned due to lack of promise. These are all detailed in his thesis document. Among them were a space-propagation algorithm, a look-up-table approach, and a symmetry exploitation algorithm. The "spaghetti style" algorithm is presently being used. However, the program is being run on a VAX, because continuously scanned still frames are still the state of the art.

When video rate computation becomes necessary, the computer running the program will become the Connection Machine 2.

3.4 Design and Information Considerations

Joel Kollin detailed in his thesis the initial design of the MIT holographic video receiver. Over time, the display evolved to a design analogous to the Scophony design(see Figure 3.1). Although the system was never fully operational, a great deal of progress was made by Kollin.

3.4.1 Interface Requirements

Kollin choose to use an RS-343 compatible Symbolics Lisp Machine frame buffer as intermediate storage. Software modifications and custom hardware reformatted the regular output of the frame buffer in order to yield a 40960 x 96 pixel window. The 40960 figure allowed for some oversampling in the horizontal direction. Through the use of this frame buffer, a 10 Hz frame rate would be possible. The Lisp Machine was chosen because it has a software configurable frame buffer, but this feature was not exploited until later.

3.4.2 Optical Engineering

The AO modulator together with the rotating polygon achieved horizontal deflection. Vertical deflection was performed by the scanning galvanometer. Lenses shrink the size of the image by a factor of 10. The output was thus a “continuously scanned” holographic video still frame.

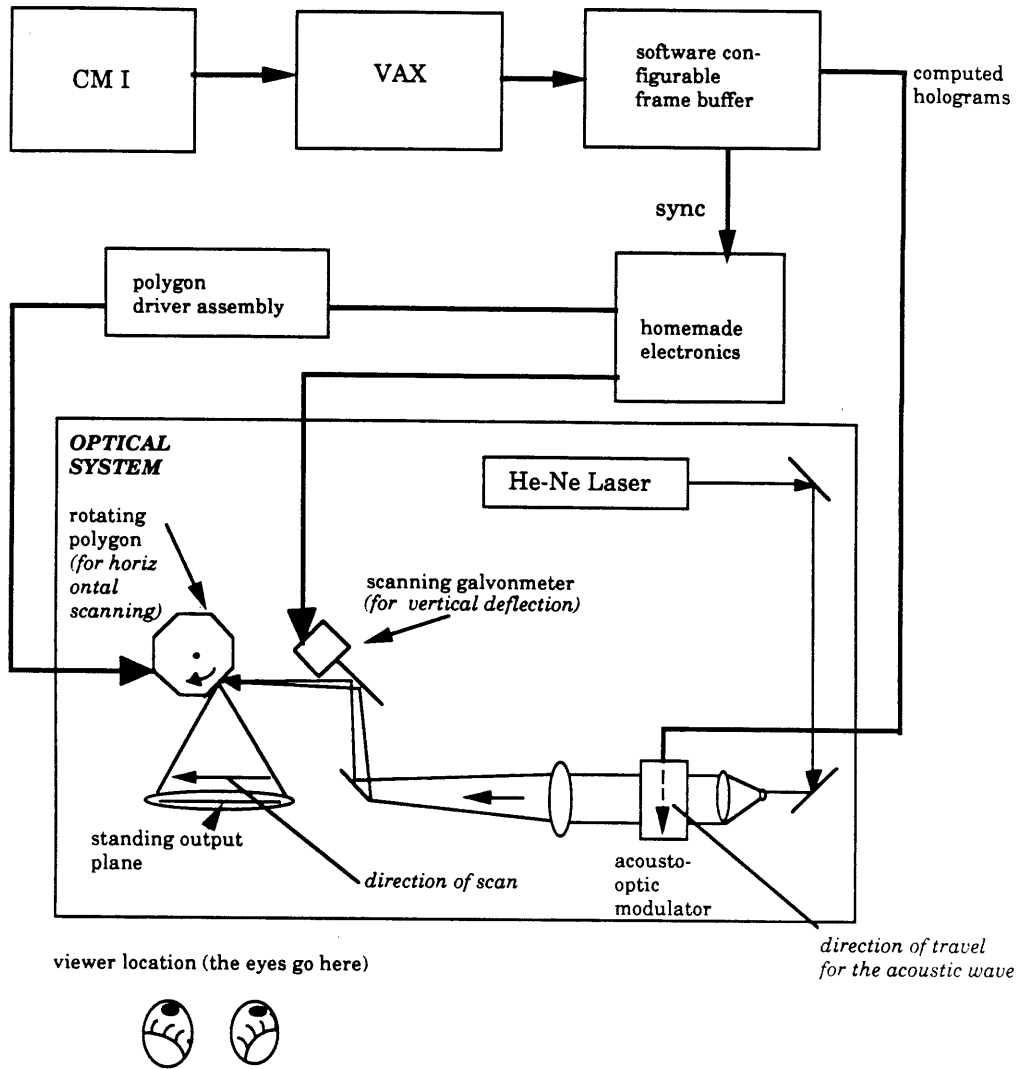


Figure 3.1: The MIT Holographic Video System as of May, 1988

The AO modulator was illuminated with a collimated beam. A simple inverted telescope was then used to de-magnify the image of the AO modulator by a factor of 10. This reduction was necessary because the resolution of the acousto-optic crystal was not as fine as required by the display. The image moving across the AO modulator at the speed of sound is made visually stationary in a way analogous to the Scopphony system method. A polygonal mirror is placed in the optical path of the imaging system and rotated in the opposite direction at a speed corresponding to the acoustic wave traveling across the AO modulator. Because the modulator crystal isn't long enough to display all the 40000 elements of one horizontal scan line at once, the rotating polygon has to abut images of the crystal against one another.

Vertical deflection is achieved with a scanning galvanometer. All the frame buffer post-processing electronics which drive both the rotating polygon and the scanning galvanometer were designed and built at the Media Lab.

The acousto-optic modulator was chosen because it appeared to offer the easiest method of display design. All other alternatives considered at that time involved device fabrication and thus required a clean room. This AO approach seemed to be an almost "off-the-shelf" way to achieve holographic video. TeO_2 was the crystal material of choice because of its high time-bandwidth product. The speed of sound for slow shear waves is .617 millimeter/ μ second in this material. This slow shear wave and high useful bandwidth (50MHz) make TeO_2 a promising candidate. Mercurous chloride and mercurous bromide promise better performance but are not yet commercially available.

An eight sided polygon would give a 90 degree sweep per image. Imaging this sweep is difficult because it requires a flat field scan lens. Quality F/1, flat field scan lenses are not made by any known manufacturer.

3.4.3 System Performance and Recommendations

Jittery, unsynchronized holographic video line images appeared in early May 1988. Some observers felt that the images had depth. Synchronization problems were suspect, but no time was available to check the system further. The small viewing zone and poor optics also obscured the analysis. Kollin concluded that the next steps would be to make the system more robust, and then to attempt a fully 3-D hologram. He anticipated the need to redesign the optics and use a more appropriate polygon scanner. He also suggested the construction of a dedicated high-speed frame buffer.

3.5 The Proposal For This Thesis

While the system described above may have displayed “holographic images”, the actual output images bore only dubious resemblance to the input image design. The system was de-bugged and reconfigured during the summer and early fall of 1988, and several design errors were discovered.

A stroboscope revealed that the rotating polygon was quite jittery; it did not rotate smoothly and with precise constant velocity. The sync signal driving the polygon was not of constant frequency. The bandwidth of the frame buffer was found to be only half of what the system required. The polygonal scanner was discovered to have 10 rather than 8 facets! The signal was processed incorrectly by the custom electronics. Extra (irrelevant) images were produced by the uncoated collimated optics. A change of the entire optical and computational strategy was needed. The

goal of this thesis was the exploration of many improvements to the system.

- making the system capable of 3-D display
- allowing for greater experimentation through increased flexibility
- creating a larger window
- achieving a faster frame rate
- exploring computation algorithms
- designing an optical distortion correction scheme

A holographic video system must display 3-D images. The system to date had displayed a 1-D horizontal hologram that projected an image out into another dimension; the resultant holographic image, then, has perceptible depth. The image is therefore 2-D. Similarly, a 2-D hologram can project a 3-D image. Some formatting software had to be written in Lisp, and the post frame-buffer electronics which drive the scanning galvanometer had to be improved and re-implemented.

Flexibility for connection to other input systems was deemed imperative if the system was to be a true research tool. For example, two systems that extract 3-D databases from video camera data exist in the Media Lab [12]; provisions should be made to allow their use as input into the holographic video system. Such investigations could offer a wide range of interactive tools that offer immediate 3-D input and display without the annoyance of "3-D" glasses.

A larger and higher resolution window was hoped for. The advantages are obvious.

A more efficient algorithm for computing the holograms was called for. Presently the computation is done in a brute force manner; no approximations are made. Several algorithms will be proposed. A Connection Machine 2 was to allow both the

computation and transmission of holograms in real time. Reasons why this has not yet been accomplished will be detailed.

Distortion caused by the lens system were determined to be extreme. Attempts were made to minimize these distortions. Possibilities for further improvement will be explored.

The remaining part of this document details the results of the investigation outlined here.

Chapter 4

System Improvements

4.1 Introduction

The holographic video system required many improvements to reach a functional state. Control of the frame buffer, and the system in general, was imperative. A major feature of holography is its three-dimensionality, so the system obviously had to be made capable of projecting 3-D images! The more quickly sequential 3-D images could be projected, and the larger these images could be made, the more realistic would be the depiction of the imaged scene. An unwanted “twin” image was eliminated through the use of a convergent reference beam. Additionally, both hardware and software issues discussed in this chapter deal with the varied concerns of faster computational time, optical distortion correction, and elimination of electro-mechanical components.

4.2 The Frame Buffer

A frame buffer is a piece of hardware, usually a circuit board housed within a computer, that is responsible for transmitting image information to a display device, generally a CRT. In a CRT, the deflection of the electron beam by magnetic coils allows the beam to scan across the phosphor coated output screen. The temporal modulation of frame information allows the pixel corresponding to time t in the scan to be turned all the way “on” and the pixel that corresponds to time $t + 1$ to be turned to a specified grey scale level. When the electron beam completes the “scan” of one frame, the beam must move back into its starting position in order to begin the scan of the next frame. This “re-positioning” takes a finite amount of time. The frame buffer uses this time to “load” in the information corresponding to the next frame. If the CRT displays n horizontal scanlines then this “re-positioning” time can be described as a fraction of n that shall be referred to as m ; manufacturers almost always specify this fraction to be an integral number of scanlines.

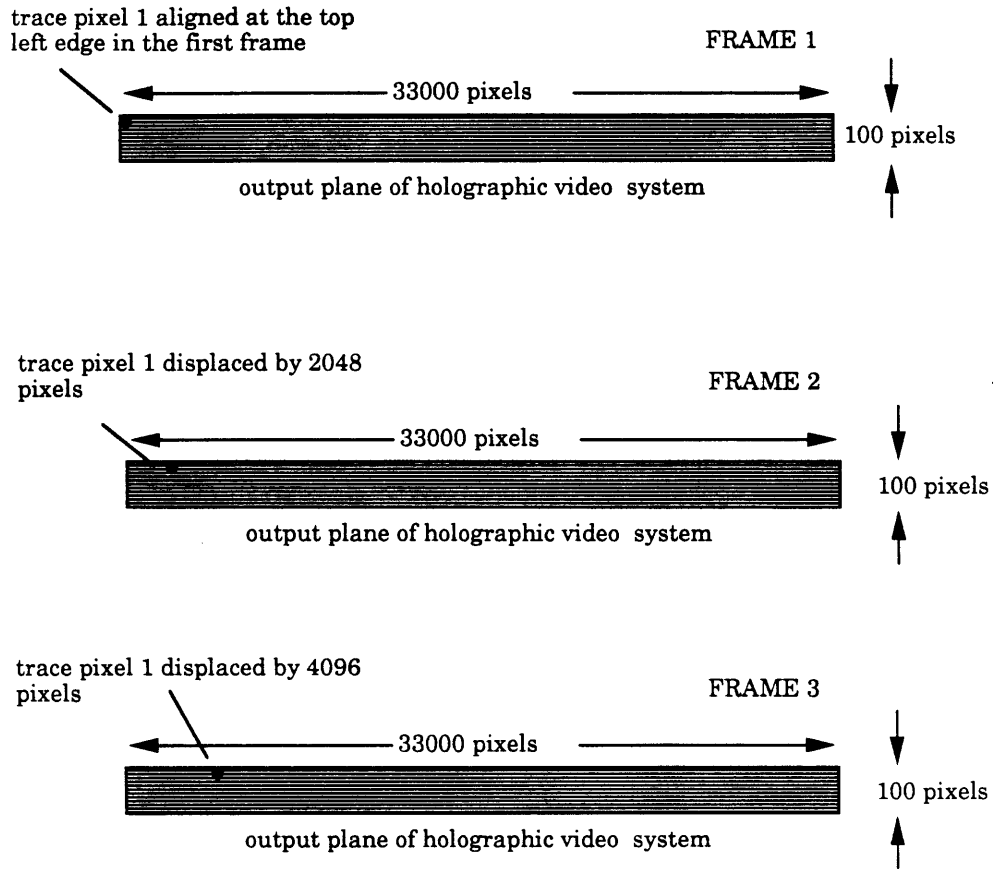
The holographic video horizontal scanline must be at least 32,000 pixels long. The only frame buffer available for this project, that is capable of accommodating the required data rate of 100 MHz, apportions scanlines to be 1 kilo-pixel in length. The frame buffer chosen is software configurable, however hardware design prevents the achievement of frame buffer defined scanlines of 32,000 pixels long. Post-processing frame buffer electronics were designed and built within the Media Lab. This hardware, among other performed functions, divides a synchronization signal transmitted from the frame buffer by a factor of 32. For every 32 “sync” pulses received, 1 is transmitted to the holographic video system. In this manner the 32 frame buffer defined horizontal scan lines can be made into one 32,000 element long scanline by the holographic video system.

However, while the “re-positioning” time of the CRT is an integral number of frame

buffer defined horizontal scanlines, it is not an integral number of holographic video defined horizontal scanlines. As a result, the position of a pixel in one frame is shifted in the next frame and so on (see Figure 4.1). A pixel's spatial position does not remain constant. The grand total $n+m$ of frame buffer scan lines was determined to be 1086, just 2 shy of a number divisible by 32. The software claims that a variable "total-vertical-lines" equals 1072. Inspection with an oscilloscope revealed that the variable "total-vertical-lines" did not refer to the quantity $n+m$. In fact, the exact meaning of this variable, as well as the meanings of other variables used in the software, remains unclear, but through some clever manipulation the author was able to add 2 more horizontal scan lines and thus alleviate the pixel "drift" phenomenon. Dave Dyer, who wrote the software that controls the software configurable frame buffer, helped make this feat possible by supplying further documentation not regularly available from Symbolics. Parameters, for example the writing speed of frame buffer, had to be changed in order to change the quantity $m+n$. A balance had to be achieved between many parameters in order to get any output at all. The output could then be evaluated with an oscilloscope, or the holographic video display itself, to ascertain its quality. This iterative approach finally proved successful and the quantity $m+n$ was increased by 2. More software was written that allows new changes to be made with greater ease.

4.3 Control

Precise control of the frame buffer is crucial to the system. The most difficult part of the design is the delicate synchronization between the AO modulator and the rotating polygon. The speed control called for here is stringent. The precise analysis will be included in the next chapter. Suffice it to say for now that balance between the speed of sound in the AO modulator with the angular velocity of the rotating



In each successive frame all of the pixels, not just pixel 1, are displaced by the same amount. The result is a total lack of continuity from frame to frame, and only 1 in 1600 frames will appear in the way in which each frame has been designed to appear.

Figure 4.1: Re-Positioning Error From Frame t to Frame $t + 1$

—

polygon, the other component capable of motion in the system, must be achieved.

To allow a range of possible frequencies to be expressed by the rotating polygon, the polygon's driving electronics required improvement. The polygon motor and driver had been designed to spin at a fixed speed, which was different from the fixed speed required by the holographic video system. The driving electronics were improved so that the achievement of the desired fixed speed was possible. However, the degree of velocity stability at this speed later proved to be inadequate.

4.4 Converging Reference Beam

The computational and optical design strategy was completely changed. A converging reference beam was substituted for the formerly collimated type. Because this holographic image is only slightly off axis, it was felt that the dubious output could be attributed to the presence of the same "twin" images that are present in Gabor holograms. The software was improved, and the optical design was upgraded. The reference beam now comes to a focus just outside of the viewing zone.

4.5 3-D Implementation

The initial 3-D design called for the addition of a vertical deflector, specifically a scanning galvanometer, to the system. An error in the 2-D version of the system became apparent when the scanning galvanometer was added. What formerly appeared as image points in the 2-D case, were spread into sinusoids of one period duration in the 3-D version of the system. This effect is an artifact of wobble in the polygon assembly. The wobble occurs because the polygon is not mounted exactly perpendicular to the motor shaft. As a result, the polygon is slightly "tilted". As the motor

shaft spins the error is transposed into the vertical displacement of images reflected from different polygonal facets.

Additionally, in the 3-D implementation, hunting (lack of velocity stability) in the motor became more apparent. Testing was performed to determine whether the hunting derived from the input signal, the polygon driver, the polygon motor assembly or the scanning galvanometer. It was determined that the bearings in the polygon motor assembly were the greatest single contributor to this problem.

4.6 System Flexibility

System flexibility was accomplished by the achievement of precise control over the frame buffer. Furthermore, the optics were designed to allow focal length and aperture alterations over a limited range. New lenses can also be substituted into the system with ease.

4.7 Larger Window/Faster Frame Rate

The attempt to achieve a larger window was postponed in favor of progress toward a video-rate system. Any additional speed garnered from the use of the Media Lab's new model of the Connection Machine, The Connection Machine 2 (CM2), will be applied to this attempt. The system, to date, has not been hooked up to the CM2. Some provisions for frame buffer reconfiguration have been made; the total number of horizontal scanlines $m + n$ can be changed to a number divisible by 32. However, the frame buffer itself has half the bandwidth of the current frame buffer. The video industry uses the term "cycle" to mean one pixel, in optics a "cycle" would denote 2 pixels, one "on" and one "off" (a linepair). Thus, a 100 MHz frame buffer rated in

video industry terms translates to 50 MHz when analyzed "optically". Currently, a 100 MHz frame buffer is being used; a useful bandwidth of 50 MHz is resultant in the display. The 50 MHz frame buffer of the CM2 will yield 25 MHz in the display. Half of the useful bandwidth of the AO modulator will go unused. One scheme devised in hopes of remedying this problem bypasses the frame buffer all together and operates on the "raw" data.

While a 30 Hz frame rate is the video standard, the current system configuration's maximum attainable frame rate is far below this benchmark. The Lisp Machine requires 5 minutes to load a frame into the frame buffer. Once the frame is in the buffer, a holographic video refresh rate of 20 Hz can be achieved. Once the move to the CM2 is made, the actual frame rate should increase because the Connection Machine 2 is order of magnitudes faster than the Lisp Machine. However, the frame buffer of the CM2 will decrease the current update rate by a factor of 2; the currently used frame buffer is twice as fast as the CM2 frame buffer. A fast update rate without a fast frame rate is somewhat meaningless if realistic animation is the ultimate goal of the system. In any case, the CM2 hook-up is eminent, and experiments will soon begin.

4.8 Computational Issues

The computational issues were examined in great detail. None of the schemes described below have yet been implemented. The opportunity to realistically simulate the actual physics of holography available only because access to a Connection Machine is available. No approximations are made. While it is educational to start the investigation in this way; an examination of the literature in the field shows many paths which may lead to a reduction in the complexity of the calculations.

Obviously, a 3-D holographic video system is the goal of this work, not the 2-D Fraunhofer diffraction regime hologram described in the early part of Chapter 2. CGH literature uses the term 2-D hologram to refer to a hologram imaging a 2-D plane at a given distance z away from the hologram plane. The term 2-D hologram also refers to a line hologram (1-D) that is capable projecting an image into the z dimension in order to display depth. The distinction between these two "types" of 2-D holograms is always made clear in this thesis. Additionally, a stereogram, in some senses, is just a 2-D, Fraunhofer diffraction regime hologram; yet a stereogram appears to be 3-D. If a series of 2-D perspective views of a 3-D database were graphically rendered, as is traditionally done in stereogram making, then computation of the more complicated Fresnel diffraction model, the computation currently being performed, could be avoided. For a 12 degree angle of view over a 125 mm viewing zone, 32 rendered views are called for, allowing for 4 mm per rendered view.

Several computer generated stereoscopic approaches to 3-D display have been explored in the literature. It seems straightforward enough to adapt one of these schemes [30] [31]. The adoption of these algorithms to holographic video will be analyzed in the next chapter.

The CGH literature details a substantial amount of work in the field of CGH signal-to-noise ratio (SNR) analysis. The conclusions made by researchers in this field should be heeded in the design of the holographic video display. The signal to noise ratio is usually defined as:

$$\text{SNR} = \frac{\text{average intensity in the desired image}}{\text{mean square error}} \quad (4.1)$$

The originally desired image is then obtained if the hologram has recorded the complex wavefront in an ideal manner with no errors. The SNR as well as the diffraction efficiency of a hologram is reduced by the amount of error introduced in various

stages of hologram production. Sources leading to poor SNR are:

- sampling errors (spatial quantization)
- quantization error (modulation quantization)
- representation related errors (aperture size and detour phase errors)
- distortion errors caused by the non-ideal behavior of the display device

Because the computed holograms used for the MIT system are sampled at or above the Nyquist limit, there is no appreciable error due to sampling. Reconstructed images do not overlap; a clean image results. Quantization error plagues most research in the field of binary CGH, but with 8 bits per pixel available in the MIT system, the error accrued is minute. After the hologram has been quantized, CGH data is usually transformed into geometric shapes for plotting. This transformation is responsible for representation error. The MIT system requires the amplitude modulation of the hologram onto a carrier frequency in order to activate the acousto-optic modulator in a regime of relatively high efficiency and linear response. This representation causes error, because the baseband signal extends into the modulated region. Only 10 percent of the modulated signal is affected, but this error sizably increases the SNR in that region. Lastly, distortion errors in conventional CGH work are caused by the positioning inaccuracy of the device plotting the hologram. Such distortion errors in the MIT system are caused by both the velocity instability of the rotating polygon and the lens distortions in the imaging system. Both of these imperfections affect the system accuracy in writing the hologram at the output plane. Distortion error is by far the single largest contributor to poor SNR in the MIT holographic video system.

After the stereographic approach to hologram computation can be demonstrated by the system, the next step in designing the ultimate holographic receiver will be the development of an **optical** method for computing the Fourier transforms required

by the stereographic approach. The amount of computation time could then be drastically reduced. An optical Fourier transform simply amounts to sending light through a lens; the Fourier transform appears at the focal plane of the lens. A feasible scheme for implementing this new design is detailed in the following chapter.

4.9 Distortion Correction

The optical distortions in the system proved to be severe; eyes moving laterally across the viewing zone perceived the object translating in the opposite direction. Clearly, research on distortion correction was called for. Perhaps this correction could be accomplished in the computational step; perhaps a predistortion technique capable of compensating for the optical distortions incurred by the system could be created [50]. However, the more nearly ideal solution is to merely increase the number of facets on the rotating polygon. The required lenses would no longer have to be as powerful. The more powerful the lens, the greater the field curvature and the more difficult this distortion correction becomes [53]. Symmetry can not be exploited in order to compensate for this effect, because the optical system also behaves like an inverted telescope, reducing the size of the image by a factor of 10. However, the use of weaker optics, possible via an increase in polygonal facets, should alleviate the severity of the incurred distortion. The new optical system was designed and a new rotating polygon assembly has been ordered, this assembly will not arrive until mid-July. As a result, the new system can not yet be evaluated.

4.10 Additional Improvements

Additionally, it seems obvious that the elimination of the electro-mechanical components would result in a much more robust system. Many schemes are possible. Again, the most straightforward approach would be to follow what others have done in the past with acousto-optic television systems. A scheme is detailed in the next chapter that shows how the replacement of the rotating polygon and the scanning galvanometer with AO modulators is possible.

Substantial progress towards the development of a functional holographic video system was made (refer to Figure 4.2). The frame buffer, a major obstacle in the development of the system, was explored and brought under control. Control of the crucial system timing via the frame buffer was made possible. A convergent reference beam was introduced, which eliminated the imaging of an unwanted twin image. A 3-D system implementation was attempted on several occasions; the results of these trials led to the discovery of a severe electro-mechanical problem in the rotating polygon assembly. A new rotating polygon has been ordered. The specification of this polygon was tailored around alleviating the severe optical distortions that also plagued the system. Computational issues were explored and several new system designs, based on the stereographic approach to holography, will be proposed in the following chapter. Additionally, alternative methods to electro-mechanical scanning were investigated, a scheme will be proposed in Chapter 5.

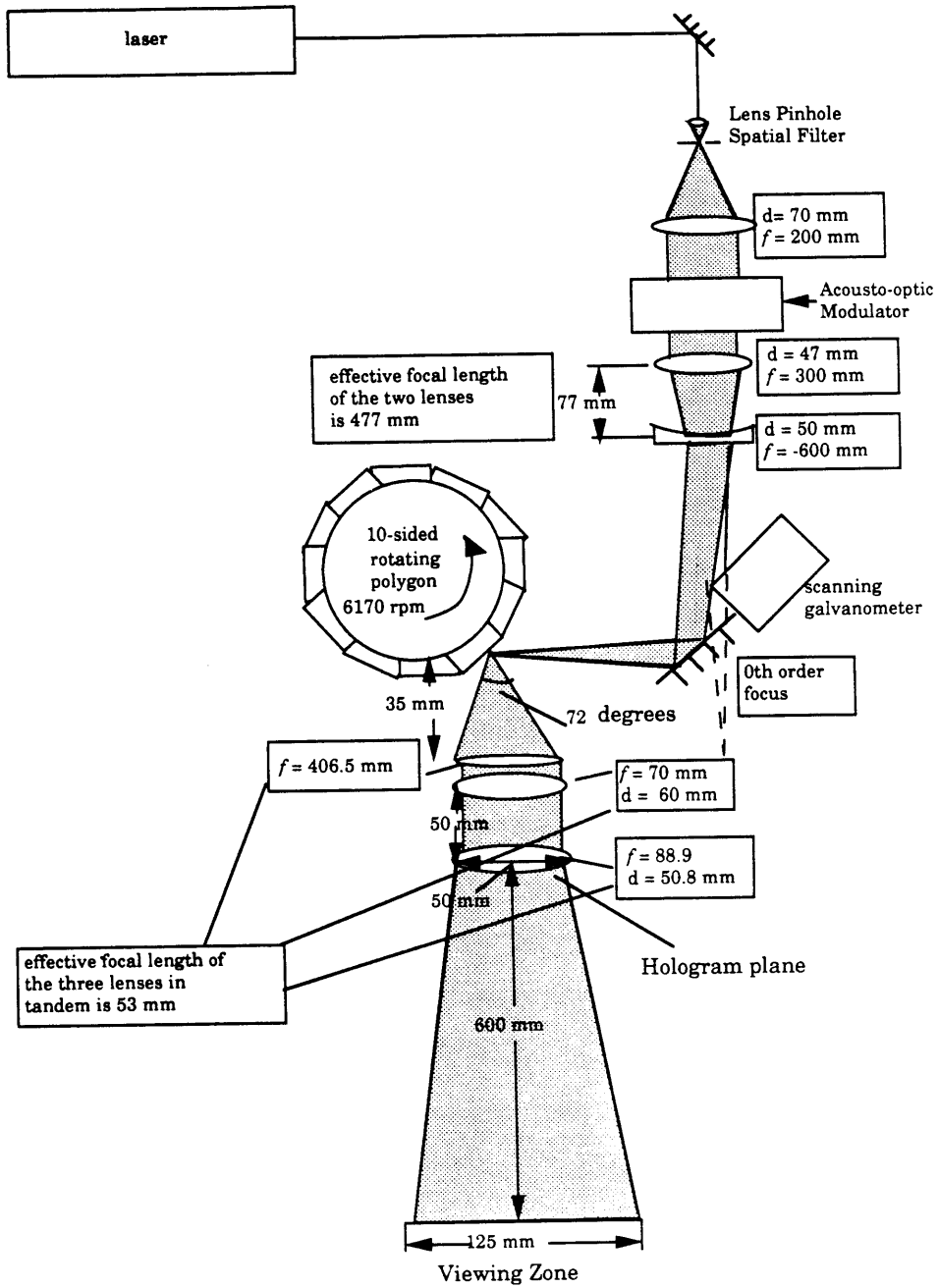


Figure 4.2: The Current Configuration of the Holographic Video Display Device

Chapter 5

Theoretical Analysis

5.1 Introduction

The system heretofore described is now theoretically analyzed. Proof of its ability to display holographic images is given. Additionally, plausible new systems are proposed. One such system solves the electro-mechanical instability problem through the elimination of all the electromechanical parts. Two other proposed systems substantially reduce the complexity of the computation required, and therefore increase the attainable frame rate.

5.2 Analysis of Present System

The mathematical proof detailing the theory of the holographic system heretofore described in this text is given.

(Refer to Figure 5.1) Let L' equal the distance between the imaged hologram and the polygon. Let d equal the length of the AO modulator. Let v equal the speed

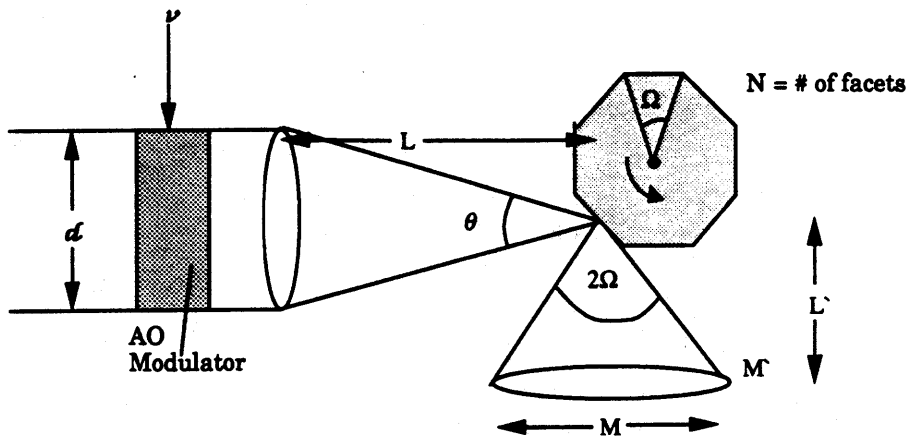


Figure 5.1: The Holographic Video System (Simplified for Mathematical Analysis)

of the acoustic wave traversing the AO modulator. L is the distance from the AO modulator to the polygon. θ is the angle subtended by the AO modulator on the polygon. ω is the angular speed of the polygon. Ω is the angle subtended by each facet. N is the number of facets. G is the magnification factor desired to increase the size of the AO modulator's image at plane M' . M is the size of the image at plane M' .

From classical elementary dynamics:

$$v = L \frac{d\theta}{dt}. \quad (5.1)$$

For the waves to traversing the Acousto-Optic Modulator to appear steady:

$$\omega = \frac{1}{2} \frac{d\theta}{dt} = \frac{v}{2L}. \quad (5.2)$$

The 2 is introduced in the above equation because the range of the angle reflected by the polygon is twice the input range. The hologram in plane M' will be composed of p "subholograms". A subhologram is the part of the entire hologram that can exist on the AO modulator at any given time.

$$p = \frac{\text{the total number of pixels in one horizontal scanline}}{(\text{video rate}) \times d/v} = \frac{MG}{d} \quad (5.3)$$

A larger scanline requires more subholograms. During the time of travel of 1 polygonal facet the whole surface M' must be covered with p subholograms. The time of travel for one facet "scan" is:

$$\tau = \frac{\Omega}{\omega} = \frac{2\pi}{N\omega} \quad \text{because} \quad \Omega = \frac{2\pi}{N}. \quad (5.4)$$

Each wave launched takes d/v seconds to traverse the length of the AO modulator. To get p subholograms, each scan must take:

$$\frac{dp}{v} = \tau = \frac{2\pi}{N\omega}. \quad (5.5)$$

Using Equation 5.3 and Equation 5.5:

$$\text{speed of motor in rpm} = \frac{\omega}{2\pi} = \frac{v}{NMG} \quad (5.6)$$

And then using Equation 5.1:

$$L = \frac{MNG}{4\pi} \quad (5.7)$$

As the motor speed and the focal length L are the two most adaptable parameters in the system, 5.6 and 5.7 are the crucial equations used in the system design. These equations are now applied to the system as it presently exists.

A 10 sided polygon was used. The AO modulator was composed of TeO_2 . This material makes possible the highest time-bandwidth product commercially available. The AO modulator is 30 mm long; this extreme length was required by the very first system design. However, the evolution of the system has made this considerable size both excessive and extravagant, although possible expansions to this system can make le use of this length. The hologram in plane M' demands to be 50 mm long. The speed of sound in the crystal is .617 mm/microsecond. The video rate is 67.9 pixels/ μ second.

$$.617 \text{ mm}/\mu\text{second} \times \frac{1}{67.9} \text{ pixels}/\mu\text{second} = 9.0 \mu\text{m}/\text{pixel} \quad (5.8)$$

The achievement of a minimum of 32,000 pixels across the 50mm output plane is required. This accomplishment will yield $1.5 \mu\text{m}/\text{pixel}$. Unfortunately, the polygon presently in use will not rotate fast enough to meet this requirement. The ability to reconfigure the frame buffer in order to slow the data rate is also limited. Therefore, the horizontal scan line became 65 kilo-pixels across the output plane M' . A resolution of :

$$\frac{65536}{50} \text{ pixels}/\text{mm} = .76\mu\text{m}/\text{pixel} \quad (5.9)$$

$$\frac{9.0\mu\text{m}/\text{pixel}}{.76\mu\text{m}/\text{pixels}} = 12 \quad (5.10)$$

is desired: a 12X reduction. Introducing the above figures into Equation 5.6:

$$\text{speed of motor in rpm} = \frac{60 \text{ sec}/\text{min} \times .617 \text{ mm}/\mu\text{second}}{10 \text{ facets}/\text{rotation} \times 50 \text{ mm} \times 12} = 6170\text{rpm} \quad (5.11)$$

The rotating polygon presently in the system is capable of this speed. Now,

inserting the known figures into Equations 5.7 to determine the optimal focal length:

$$L = \frac{10 \times 50 \times 12}{4\pi} = 477.5\text{mm.} \quad (5.12)$$

Unfortunately, the 3 degree spread of the acousto-optic modulator over 477.5 mm is 25mm. The length of each facet is just 12 mm. Clearly a larger polygon is needed. As long as a larger polygon is being sought, it makes sense to use this opportunity to alleviate the severe optical distortion and velocity instability problems. With a 10 sided polygon, the final lens in the system must be faster than an F/1 lens. As one moves laterally from left to right in the viewing zone, the image at plane M' appears to move in a semi-circular fashion in the opposite direction; this phenomenon is called *field curvature*. The image is distorted from one viewpoint with respect to another viewpoint, and it becomes difficult to perceive the three dimensionality of the imaged object. In order to eliminate this undesirable effect, a polygon with more facets is required. A new polygon has been ordered with N facets. In the present system configuration, it is difficult to determine whether or not the image is really 3-D. When one's eyes are placed equidistant from the center point in the viewing zone, the 3-D-dimensionality is apparent. As described above. when one moves one's eyes laterally back and forth the image distorts. The distortions are, in fact, so severe that the viewer remains unconvinced as to whether they are viewing merely optical distortions or, in fact, a real 3-D holographic video display. However, some stereo-pairs that exploit the symmetry of the field curvature have been photographed. The inclusion of these stereo pairs in this thesis was not possible. Only a set of photographs or slides can allow the viewer to detect the projected images against the very noisy background created by the severe electro-mechanical instability of the rotating polygon and poor optical design.

To remedy the problem of distortion, the simplest solution is the elimination of the stringent requirements on the optics. As long as a new polygon is required the

number of polygonal facets, as well as the size of each facet, should be increased to the largest polygon assembly commercially available. The candidate is an 18 faceted polygon with 25.4 mm per facet. Solving for equation 5.6 and 5.7:

$$\omega = \frac{60 \times .617\text{mm}/\mu\text{s}}{(18\ 50\ 6)} = 6856 \text{ rpm} \quad (5.13)$$

$$L = \frac{(18\ 50\ 6)}{4\pi} = 429.7\text{mm} \quad (5.14)$$

The focal length of 429.7 mm allow the 3 degree range of AO modulation to spread 22.6 mm. The polygonal facets on the new polygon are 25.4 mm long. A good hysteresis synchronous motor capable of rotating at 6856 rpm and synchronizing to the external frame buffer derived sync signal is required. This type of motor is needed in order to achieve good velocity stability. See Figure 5.2 for a complete diagram of the redesigned setup.

It is important to note that the image carrying signal cannot be sent directly to the AO modulator, as this video signal occupies a bandwidth of 0 to 50 MHz and the AO modulator has an operating band of 45 to 95 MHz. Amplitude modulation of the signal into this region is necessary, but this process incurs errors. The highest 5 MHz of the baseband signal creates noise in the transmitted signal. Limitation of the frequency extent of the baseband signal to 47.5 MHz is necessary. In addition, only a small difference between the frequency of the baseband signal and the carrier frequency exists. For this reason, a clear cut "envelope", as is normally perceived in amplitude modulation, becomes difficult to detect (see Figure 5.3). The attempt to transmit a regular 2-D video signal would result in severe high frequency "noise" in the image. Luckily, the system being discussed transmits a holographic image. The high frequency "noise" is thus easily separated from the holographic image; the "noise" is diffracted into the outer limits of the viewing zone. The major effect is a reduction in the efficiency of the hologram. Because the viewer essentially peers into an only somewhat diverged laser beam, not much power is required in the first

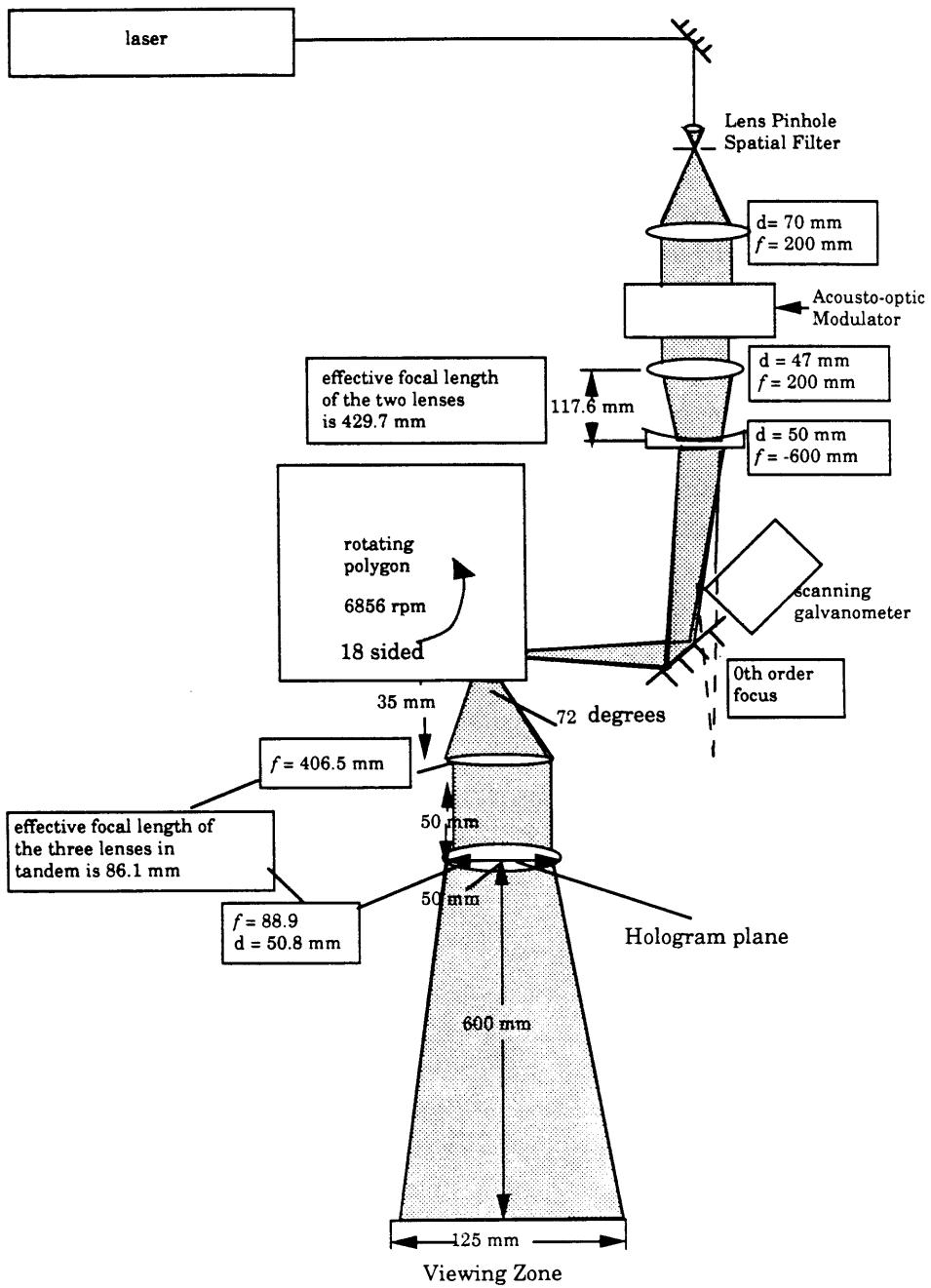


Figure 5.2: New Holographic Video Setup Using 18 Sided Polygon

place. The system doesn't have to be very efficient. However, a weaker signal creates a lower SNR, effectively highlighting any noise present in the image.

5.3 Proposed Elimination of Electro-Mechanical Parts

Although the original Scophony design used electro-mechanical components, these were quickly replaced with electro-optic components that performed identical functions. Subsequent acousto-optic TV's have also relied on electro-optic components rather than their electro-mechanical counterparts [40], [46], [44], [44]. Perhaps this substitution may be performed on the holographic video system.

Recall that the holographic image has a 50 MHz bandwidth. TeO_2 also has a 50 MHz bandwidth. TeO_2 is therefore capable of displaying this image. In order to multiplex the p subholograms together, the bandwidth of the AO modulator replacing the rotating polygon would need to be $(p \times 50)$ MHz. Using Equation 5.3:

$$p = \frac{32768}{(30 \text{ mm})(1/.617 \text{ mm}/\mu\text{second})(1024/15.07 \text{ pixels}/\mu\text{second})}, \quad (5.15)$$

$$= 9.9 \text{ subholograms}, \quad (5.16)$$

$$(9.9 \text{ subholograms}) \times (50 \text{ MHz}) = 495 \text{ MHz}. \quad (5.17)$$

No commercially available AO modulator exists with such a high time bandwidth product. However, suitable new materials are being developed, and these materials may become commercially available before long. If such a material could be obtained by the MIT Media Lab, the following proposals could be realized.

The length of this modulator can be quite short, as well with the length of the TeO_2 . The variable p in the above calculations makes it appear that the actual length

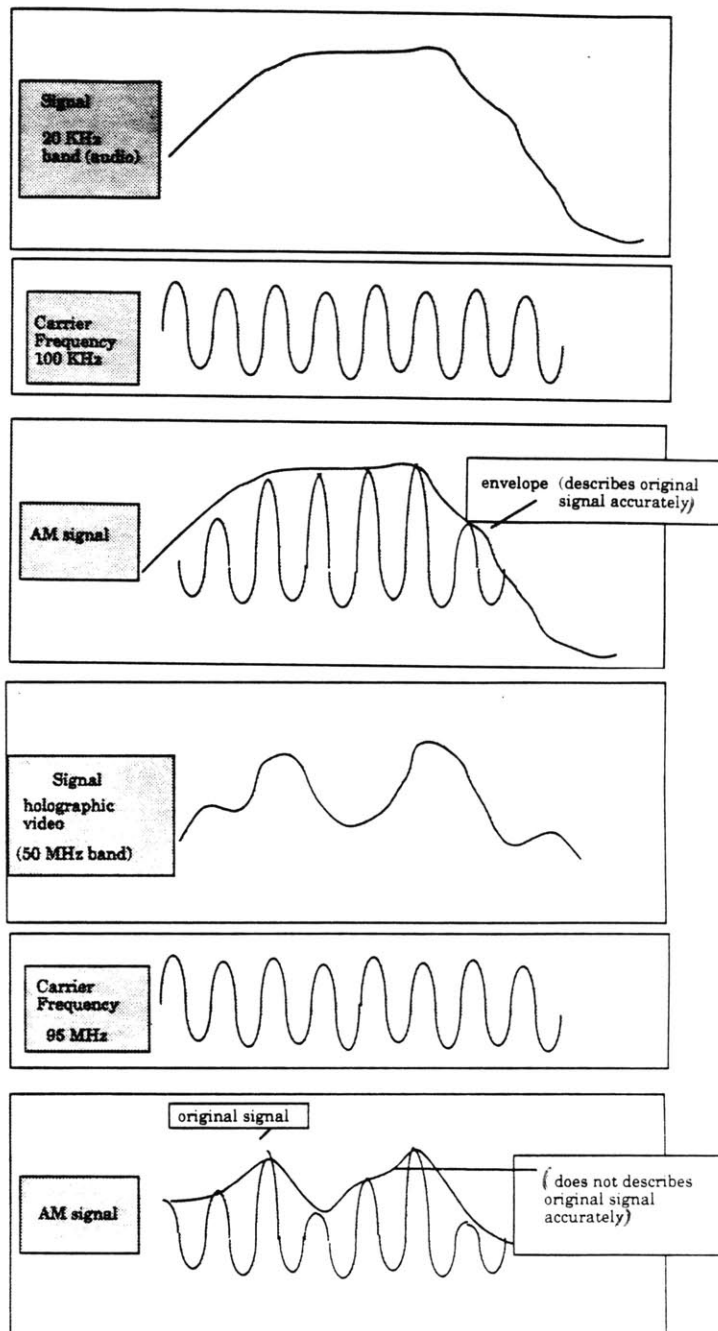


Figure 5.3: AM Envelope Detection

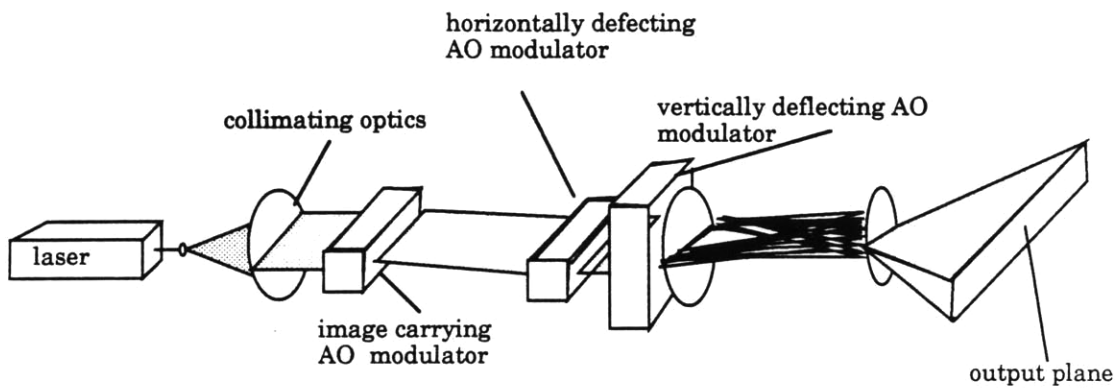


Figure 5.4: Proposed Elimination of Electro-Mechanical Parts

of the crystal is important. What p really relates is the spatial frequency of the AO modulator, through the incorporation of the speed of sound in this medium, with the pixel rate of the signal being sent to the modulator. The size of this modulator only effects the efficiency of the imaging system, in a manner similar to Scophony (see Equation 2.25).

The high-bandwidth modulator, which shall subsequently be referred to as the scanning modulator (SM) requires an electronic control signal that linearly ramps over a 495 MHz range (see Equation 5.17). This ramp must be repeated for every scanline; scanlines in the originally specified window configuration occur every:

$$32 \text{ scanlines} \times 15.07 \mu\text{seconds/scanline} = .48 \text{msec} \quad (5.18)$$

or at 2073 Hz. This ramping must then be done at a rate of 2.073 KHz.

5.3.1 The Optical Design

Note that the 2 final lenses in the system no longer require extremely "fast" lenses (see Figure 5.4). They must allow a 12 degree spread of light to the M' plane as specified by the original design constraints. The light emerging from the scanning modulator has an angular field of play:

$$m\lambda f = \sin(\theta) \quad (5.19)$$

$$\sin^{-1}((330 \text{ lp/mm}) (633 \times 10^{-6})^{-1}) = 12 \text{ degrees.} \quad (5.20)$$

As is apparent, the achievement of the angular field of play is not problematic, as was the case with in the electro-mechanical design. If it ^{were} possible to manufacture a 60 faceted polygon where each facet had a length of 200 mm, meaning that the polygon would have a 4 meter diameter, then the output angle would also be 12

degrees without the use of any extremely "fast" lenses. By increasing the spatial frequency of the SM to that required by the *design* spatial frequency of 330 lp/mm the angle output increases to a maximum of 12 degrees. Lens design then becomes relatively easy.

In a more straightforward manner, an acousto-optic modulator such as TeO₂ performs the vertical deflection at the untroublesome rate of 30 Hz across a 1mm range in the M' plane. This vertical deflector replaces the scanning galvanometer. Using TeO₂ to accomplish this task is not necessary. TeO₂ is capable of 3 full degrees of deflection. The system only requires about 1 degree. A less expensive AO modulator could be employed in the task of vertical deflection.

5.4 Stereogram-Type Video Systems

The lack of ^acommercially available modulator with 10 times the time-bandwidth product of TeO₂ prevents the realization of the above proposal. This required bandwidth could conceivably be reduced through a stereogram approach. Additionally, the system itself could be greatly simplified. A 2-D rendered image takes up a much smaller frequency range than the holographic images presently being used. As derived in Section 4.8, 32 2-D un-centered rendered views would be needed for the 125mm viewing zone: this configuration allows each "slit" 4 mm in extent. In order to allow use of the new 18 sided rotating polygon assembly, let each image be 1024 X 32 pixels. An entire horizontal scanline would then be 32768 pixels long, as 1024 pixels are contributed from each of the 32 rendered views. The rightmost view will contribute to the beginning of the scanline, the second rightmost view will trail the contribution from the rightmost view, and the leftmost view will add the final 1024 pixels to the horizontal scanline. The process will begin again with the rightmost view on next

horizontal scanline.

In a vein similar to the approach of CGH algorithms discussed in Section 2.3.4, the Fourier transforms of these rendered views are taken [30] [31]. The implementation is a straightforward extension of the both the systems previously described; in fact, the only parts that require change are the image computational strategy, the frame buffer formatting software and the post-processing frame buffer electronics.

In version 2 of this design, the Fourier transform is performed optically. This feat is accomplished via the transmission of the image through one less lens. The lens placed immediately “downstream” from the AO modulator is removed. The other system components remain in nearly identical positions.

The first AO modulator receives the electronic image signal from the frame buffer. 50 uncentered rendered views comprise this image and are horizontally separated. The width of each strip is P pixels. The total number of pixels comprising each horizontal scanline is then $50 \times P$. The optical image of the first AO modulator is *not* transmitted through a lens.

The next component of the system, a scanning galvanometer, provides vertical deflection in the same manner as the present system. The rotating polygon, the last major system component, receives input images that can now be described as rendered views, rather than the hologram itself as before. The views moving across the AO modulator are made to appear stationary in the output plane in the same method previous described in this document. The polygon travels in an opposite direction but with a speed corresponding to that of the image traversing the AO modulator. The presentation of views is similar to the presentation of rendered views in a holographic stereogram setup, however the use of AO technology increases the speed of presentation into a range where animated holograms, computed “on the fly” are possible to create. The rotating polygon coupled with the flat-field scan lens

now sweeps out these views over a 27 degree range. One facet sweeps 50 views, or one horizontal scanline. The image that appeared at the rotating polygon is Fourier transformed again so that the hologram is now swept out to plane M' which coincides with the focus of the f - θ lens system. A collimated image, such as the 50 uncentered rendered views, ^{is} ~~are~~ affected by the lens in such a way that a Fourier transform appears at the focus of that lens. M is 300 mm in length. Eyes peering into the viewing zone, also at plane M' , perceive the image projected by this animated stereogram-type holographic video system.

The hologram is created by the Fourier transform action of the lens that acts on the incoming collimated image "downstream" from the rotating polygon. This collimated beam traversing through a convex lens is brought to a focus at a distance f from the lens. f corresponds to the focal length of the lens. Assuming no absorption, the effect of the lens is to introduce a phase delay which varies across the aperture of the lens. The plane wavefront is converted into a converging spherical wavefront. This wavefront can be written as [49] :

$$\Delta\phi(x, y) = \frac{\pi}{\lambda f}(x^2 + y^2). \quad (5.21)$$

Here ϕ refers to the phase of the wavefront, λ the wavelength of light and f the focal length of the lens. A lens can be considered equivalent to a transparency with a complex amplitude transmittance

$$\tilde{g}(x, y) = \exp\left[\frac{i\pi}{\lambda f}(x^2 + y^2)\right]. \quad (5.22)$$

The collimated transmittance of the 50 abutted uncentered 2-D perspective views, which shall be referred to $t(x, y)$, is combined with the complex amplitude transmittance of the lens ^{to} yields a net amplitude ~~of~~ $t(x, y) \exp\left[\frac{i\pi}{\lambda f}(x^2 + y^2)\right]$. The complex amplitude at a point (x_f, y_f) can now be calculated and is given from the relation

[49] :

$$a_f(x_f, y_f) = \frac{i}{\lambda f} \exp\left[\frac{-i\pi}{\lambda f}(x_f^2 + y_f^2)\right] \times \int_{-\infty}^{\infty} \int_{-\infty}^{\infty} t(x, y) \exp\left[i2\pi\left[x\frac{x_f}{\lambda f} + y\frac{y_f}{\lambda f}\right]\right] dx dy. \quad (5.23)$$

or

$$a_f(\xi, \eta) = \frac{1}{i\lambda f} \exp[i\pi\lambda f(\xi^2 + \eta^2)] A_1(\xi, \eta), \quad (5.24)$$

where

$$\xi = \frac{x_f}{\lambda f}, \quad \eta = \frac{y_f}{\lambda f}, \quad (5.25)$$

and

$$a_f(x, y) \longleftrightarrow A_f(\xi, \eta). \quad (5.26)$$

Thus the incoming image $t(x, y)$ traverses through the lens and at the focal length of the lens the Fourier transform of that incoming image appears. As described in Chapter 2, the Fourier transform of an image $t(x, y)$ is a holographic representation of that image. Therefore, the hologram appears in plane M' , at the focal length of the lens.

If each rendered view is 128 by 128 pixels, a regular 1K x 1K frame buffer that updates images at 30 Hz could be used, and the holo-video rate would also be 30 Hz. However, the polygon speed would require a 4X increase; an entirely new polygon capable of this speed is then required. To avoid the need for a new polygon and to adhere to conventional storage configurations, a configuration of 512 X 64 is more feasible. Such a design was tested using the rotating polygon presently in the system, as well as the rest of the system components. The test met with limited success. The image was convincingly 3-D, although mechanical instability again contributed to poor quality. This poor quality was primarily manifested in the image resolution. The side-to-side visibility was good, far better than that of the present system. The lack of severe optical distortion is not surprising, as this stereogram-type holographic video system does not have the same stringent optical restraints as the "straight" holographic video display. The pursuit of this idea could be promising. A CM2 would be useful in both rendering and loading the required perspective views in real time (30Hz).

It seems that such a display is quite plausible. In fact, all of the systems proposed in this chapter are plausible. However, the realization of an actual fully functional system has been much more difficult and time consuming than anticipated. The original design suffered primarily from optical distortions. The implementation of this design was additionally plagued with electro-mechanical instability. These issues have been analyzed, and solutions to the problems have been proposed. The most straight forward solution involves the substitution of a new rotating polygon into the system. A brand new optical design has been tailored around this specified polygon. The post-processing frame buffer electronics will have to be modified in order to deliver the correctly timed signal to the polygon driver. The required modifications are straight forward. Two proposals have been made that alter the existing system into one that will display animated stereograms. In the first system, the only required modifications are in the software and the post-frame buffer processing electronics. The second scheme for accomplishing this stereogram-type display doesn't require the computer to compute the actual CGH, but rather the display system optically computes the CGH from a series of transmitted rendered views. Once the new polygon is substituted into the present system, modifications can be easily made that will allow the CGH to be optically computed.

It is unfortunate that most of the past year has been spent attempting to implement a design. It seems like a long time. However, significant progress has been made. The system is now capable of displaying 3-D images, albeit images that are still of very poor quality due to severe optical distortions and electro-mechanical stability problems. These problems are now understood, and can therefore be eliminated. The parts required to fix the system have been ordered. Upon their arrival a much improved holographic video system is expected.

Chapter 6

Conclusions

6.1 Improvements

Improvements to a holographic video system made throughout the academic year 1988-1989 are documented. These improvements entailed an entire reconfiguration of the control system electronics and software, a 3-D implementation of the holographic video system, the reduction of the severe optical distortion, the removal of the conjugate image usually present in this type of hologram, a proposal to eliminate the electro-mechanical parts, and the proposed design of 2 new stereogram-type holographic video systems.

The holographic video system currently displays continuously scanned still frames of 3-D images, but the optical distortions electro-mechanical instability are so severe that the three dimensionality of the display is difficult to perceive. However, stereo pairs have been successfully photographed. A new set of components has been designed and ordered that will eliminate both the optical distortions and electro-mechanical instabilities; these components have not yet arrived.

This system is the first operational holographic video system in existence. The images currently displayed on this system are the simple sums of points. However, as the system improves in the coming years, the images are destined to become more and more complex. True 3-D holographic video with the image quality of broadcast television is not far off in the future, or so we hope.

Bibliography

- [1] D. Gabor. A new microscopic principle. *Nature*, 161:777-8, 1948.
- [2] E. Leith and J. Upatnieks. Reconstructed wavefronts and communication theory. *Journal of the Optical Society of America*, 52:1123-30, 1962.
- [3] E. Leith and J. Upatnieks. Wavefront reconstruction with diffused illumination and three-dimensional objects. *Journal of the Optical Society of America*, 53:1377-81, 1964.
- [4] Y. N. Denisyuk. Photographic reconstruction of the optical properties of an object in it's own scattered radiation field. *Soviet Physics*, 7:543-5, 1962.
- [5] Y. N. Denisyuk. On the reproduction of the optical properties of an object by the wave field of its scattered radiation. *Optics and Spectroscopy*, 15:279-84, 1963.
- [6] S. A. Benton. Hologram reconstructions with extended incoherent sources. *Journal of the Optical Society of America*, 61:649, 1969.
- [7] S. A. Benton. Holographic displays - a review. *Optical Engineer*, 14(5):402-407, 1975.
- [8] S. A. Benton. Sythetic holography. *CLEO 1989*, to be published.
- [9] J. C. Boudreaux and T. R. Lettieri. Toward real-time animation of holographic video images. *SPIE*, 845, 1987.
- [10] L. D. Siebert. Large scene front lighted hologram of a human subject. *Proceedings of the IEEE*, 56:1242-3, 1968.
- [11] Stephen A. Benton. Photographic holography. *SPIE*, 391, 1983.
- [12] V. Michael Bove Jr. Sythetic movies from multi-dimensional image sensors. *Ph.D. Thesis, MIT Media Lab*, June, 1989.

- [13] J.W. Goodman. *Introduction to Fourier Optics*. McGraw-Hill, New York, 1968.
- [14] T.C. Lee and D. Gosen. Computer generated holograms. *Applied Optics*, 10:961, 1971.
- [15] W.J. Dallas. Computer-generated holograms. *The Computer in Optical Research*, 41:291-366, 1980.
- [16] R.C. Singleton. The discrete fourier transform. *Transactions of the IEEE*, 17:93, 1969.
- [17] A.W. Lohmann. *The space-bandwidth product applied to spatial filtering and holography*. Volume Tech Report IBM RJ 438, IBM Research Labs, San Jose, 1967.
- [18] B.R. Brown and A.W. Lohmann. Complex spatial filtering with binary masks. *Applied Optics*, 5:967-9, 1966.
- [19] J.W. Goodman. Some effects of Fourier domain quantization. *IBM Journal of Research and Development*, 14:478, 1970.
- [20] P.S. Naidu. Quantization noise in binary hologram. *Optical Communication*, 15:361, 1975.
- [21] W.H. Lee. Sampled Fourier transform holograms generated by computer. *Applied Optics*, 9:168, 1970.
- [22] C.K. Hsueh and A.A. Sawchuck. Computer generated double phase holograms. *Applied Optics*, 17:3874, 1978.
- [23] C.B. Burckhout. A simplification of Lee's method of generating holograms by computer. *Applied Optics*, 9:1949, 1970.
- [24] W.H. Lee. Binary synthetic holograms. *Applied Optics*, 13(4):1677, 1974.
- [25] W.H. Lee. Binary computer generated holograms. *Applied Optics*, 18:3661, 1979.
- [26] J.J. Burch. A computer algorithm for sythesis of spatial frequency filters. *Proceedings of the IEEE*, 55:599, 1967.
- [27] L.B. Lesem et al. Kinoforms. *IBM Journal of Research and Development*, 14:485, 1969.
- [28] D.C. Chu et al. The referenceless on axis complex hologram. *Applied Optics*, 12:1386, 1973.

- [29] Y. Ichioka et al. Three-dimensional computer generated holograms. *Applied Optics*, 10:10 403, 1971.
- [30] Toyohiko Yatagai. Stereoscopic approach to 3-d display using computer generated holograms. *Applied Optics*, 15 No. 11:2722-2729, November 1976.
- [31] L. P. Jaroslavski et al. Stereoscopic approach to 3-d display using computer generated holograms: comment. *Applied Optics*, 16 no. 8:2034, August, 1977.
- [32] M. D. Levine. *Vision in Man and Machine*. McGraw-Hill, New York, 1985.
- [33] W. P. Parker. *Output Devices for Electronic Holography*. MIT Master's Thesis, Cambridge, Mass, February, 1989.
- [34] Lawrence E. Tannas Jr. *Flat-Panel Displays and CRTs*. Van Nostrand Reinhold Company, New York, 1985.
- [35] R.L. Ashmore. Mechanical scanning and high definition pictures. *TV and Shortwave World*, 453-454, August, 1936.
- [36] L.M Myers. Mechanical film transmission. *TV and Shortwave World*, 369-373, June, 1936.
- [37] A. B. Lippman. Digital Video lecture. *MIT Media Lab*, 1988.
- [38] L.M Myers. The Scophony system: and analysis of its possibilities. *TV and Shortwave World*, 201-294, April, 1936.
- [39] Editor. We see scophony television: a remarkable advance. *TV and Shortwave World*, 391-393, July, 1936.
- [40] F. Okolicsanyi. The Wave-Slot, an optical television system. *The Wireless Engineer*, 527-536, October, 1937.
- [41] Adrian Korpel. *Acousto-Optics*. Marcel Dekker, New York, 1988.
- [42] Eugene Hecht. *Optics*. Addison-Wesley, Reading, Mass, 1987.
- [43] Richard H. Johnson. Optical beam deflection using acoustic-traveling-wave technology. *SPIE*, 90:40-48, 1976.
- [44] I. Gorog et al. A television-rate laser scanner 1. general considerations. *RCA Review*, 33:623-665, December 1972.
- [45] I. Gorog et al. A television-rate scanner 2. recent developments. *RCA Review*, 33:666-673, December 1972.

- [46] J.B Lowry et al. Pulsed scophony laser projection system. *Optics and Laser Technology*, 20:October, 1988, 255-258.
- [47] Richard V Johnson. Electronic focusing in the scophony scanner. *SPIE*, 222:15-18, 1980.
- [48] Korpel et. al. A television display using acoustic deflection and modulation of coherent light. *Applied Optics*, 5:1667-1682, October, 1966.
- [49] P Hariharan. *Optical Holography*. Cambridge University Press, New York, 1987.
- [50] S. A. Benton. Toward telephonic holography. *Research Proposal to US WEST Advanced Technologies*, April 1987.
- [51] Joel S. Kollin. *Design and Information Considerations for Holographic Television*. MIT Master's Thesis, Cambridge, Mass, June, 1988.
- [52] J. S. Underkoffler. *Development of Parallel Processing Algorithms for Real-Time Computed Holography*. MIT Bachelor's Thesis, Cambridge, Mass, May 1988.
- [53] Rudolf Kingslake. *Optical System Design*. Academic Press, New York, 1983.